Resource-Efficient Technologies 1 (2021) 1–38

TOMSK POLYTECHNIC UNIVERSITY

Resource-Efficient Technologies

journal homepage: http://reffit.tech

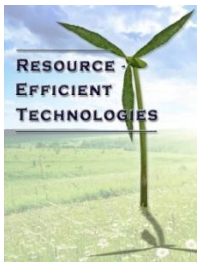

Review Article

COMPARATIVE MECHANICAL PROPERTIES STUDIES ON HEAT & UNHEAT TREATED AL7075 ALLOY HYBRID COMPOSITES

T.G. Gangadhar[a], D.P. Girish[b]

[a] Department of Mechanical Engineering, SJBIT, Bengaluru

[b] Department of Mechanical Engineering, GEC, Ramanagaram

Abstract

In the present work, Al7075 based hybrid composites was developed using stir casting technique. Al7075 hybrid composites with different weight percentage of Mica, Graphite and E-glass fiber were developed to study the effect of these reinforcements on microstructure and mechanical properties, E-Glass fiber is kept constant at 0, 2, 4 %, Mica is varied from 1–3 % in steps of 1 and Graphite varied from 1–5 % in steps of 2. It can be seen that the three peaks corresponding to Al were seen at 38º, 46º and 65º 2θ angles and small peaks related to all the three reinforcement mica, graphite and E-glass fiber were observed in the XRD pattern. Grain size analysis was examined using Clemex Image-Analyzer software, it was observed that decrease in grain size of Al7075 matrix was found to decrease with the increase in reinforcements, Hardness was found to increase with increase in reinforcement content whether it could E-glass fiber from 0–4 % or mica from 1–3 % or graphite content from 1–5 %. Ultimate tensile strength increased with the increase in reinforcement content both before and after heat treatment.

Keywords: AL7075; Grain Size Analysis; XRD; Tensile testing; BHN; Strengthening Mechanism; SEM

1. Introduction

The consumption of composite materials in every manufacturing sector has substituted the conventional resources due to their properties for instance low-weight-high-strength. Most of the conventional parts are being supplanted by composite since of the properties that they hold such as low-weight-high-strength, capacity to endure mechanical properties at elevated conditions, larger physical, outstanding tribological, high creep resistance and better-quality toughness etc. The primary idea behind any composite materials is to obtain a better set of properties than a conventional material. Thus, for any composite materials irrespective of type matrix materials used the selection of reinforcement plays a decisive character to play for obtaining the tailor made properties based on the applications [1–2]. Aluminum/metal matrix composites established an authoritative group of design and weight industrious supplementary materials that are endowing each circle of industrial applications. Currently, composites are attaining incredible acceptance over the conventional metals and alloys in numerous segments such as automobile engineering, aerospace sector and sports domain due to the circumstance that properties can be custom-made as per ones necessity- A exceptionality of composites [3–4]. Synthesis of discontinuous fiber or particles reinforced composites materials is usually associated with low manufacturing temperature and low cost with ease of manufacturing. The size, shape density, composition of the reinforce-

* Corresponding authors: Gangadhar T.G.,
E-Mail:tggangsadi@gmail.com

☆ Peer review under responsibility of Tomsk Polytechnic University.
https://doi.org/ 10.18799/24056537/2021/1/281

ment materials typically commands the ultimate physio-mechanical properties of the aluminum composites. In addition to morphology of the reinforcement, the processing means and processing conditions are important aspects for obtaining good quality composites with superior bulk properties. Popular processing techniques can be used to synthesis hybrid metal matrix composites in a conventional manner. Among all techniques, as mentioned earlier stir casting process is frequently used method for manufacturing process in view of its low cost and simplicity. Stir casting process comes under liquid metallurgy techniques [5–6]. There are appropriate heat treatment procedures available for different alloys to get desired precipitates in the matrix. The mechanism behind this strengthening is formation of coherent solute atoms which causes strain due to mismatch with the solvent atoms. When dislocations are trapped by these clusters of coherent solute atoms then the alloy is said to be strengthened. On the other hand, if the precipitates formed are semi-coherent or incoherent then they are can inhibit the dislocation motion leading to increase in strength of alloy [7]. Jamsari et al., [8] have studied the metal matrix composite with aluminum base reinforced with flyash and used SiC as the synthesizing powder. The matrix of aluminum was mixed with 5, 10 and 15 % of the synthesizing powder and was compacted at certain temperature and pressure. Mechanical properties were analyzed with incremental proportion of reinforcement. It was noted that the increment in flexural and hardness strength was noted for higher proportion of the reinforcement. 300 kg/mm^2 was the hardness that was achieved at 15 % of reinforcement and flexural strength of 107.5 MPa was noted as highest results. Jaswinder Singh et al., [9] have made a study of process ability and easiness for development of hybrid aluminum composite for application towards aerospace and automotive by cost reduction consideration. The development of composites by the method of stir casting is carried out and the characteristic study for mechanical properties is done. The process of stir casting has dispersed the reinforcements in evenly manner and the amount of porosity has been found be in the nominal range. It was noted, increment in density wit increase in ceramic reinforcement, however the reduction in density was observed to reduce with addition of flyash, rice husk, mica etc. Al/SiC/FA, Al/SiC/mica, Al/SiC/BLA, Al/SiC/B4C were the combination chosen for the study and the fabrication process was found to be in ease without any complication for any of these combinations. Hanumanth et al., [10] have also studied on the governing properties of the of the particles like the ability of the particle to exhibit wettability, rate of solidification, fluidity property of the melt, the method incorporated for mixing of the composite and the type of reinforcement. It was also noted that addition of magnesium helps in improvement of wettability property between the reinforcement and the alloy. Prasad et al., [11] carried out the microstructure study of aluminum alloy reinforced with SiC and rice-husk (RHA). The observed result showed the possibility of uniform distribution. Optimization and control of various parameters during the process of manufacturing will enhance the ability to disperse the particles evenly. Kalkanli et al., [12] compared the enhancement in the flexural and tensile strength of the aluminum composite with and without heat treatment. The adding of SiC to the aluminum increased in above mentioned properties. 10 % increase of flexural strength was noted in the case of composite without heat treatment; however there was an improvement on maximum scale in flexural strength after heat treatment. The results were noted to be similar for analysis of the properties of tensile strength. 10 wt % of SiC was used for the comparison of both the specimens. Heat treated specimens showed highest tensile strength of 350 MPa. The addition of 30 wt % of SiC to the matrix reduced the values of both flexural and tensile strength. The clustering of the SiC could be analyzed as the prominent reason for the reduction of strengths. K.K. Alaneme et al., [13] investigated the experimentally developed Al6063 reinforced with SiC composite for its fracture toughness with heat treatment. It was observed that ageing heat treatment carried out at 180 °C for a time interval of 3 hours and later water quenching it has a noteworthy impact on improvement of fracture-toughness of the composite. Song et al., [14] studied the heat treatment results of Al 2021 and Al 6064 reinforced with SiCp in the 20 volume percent which were of the size 3 and 20 μm respectively. T6 condition of heat treatment was followed for the study, which included solution treatment, quenching and pre-ageing. 530 °C for 1 hour was the temperature and time chosen for solution treatment, followed by quenching and pre ageing at room temperature for 20 hours. The ageing of material was carried out from 50 °C to 250 °C with increment of 50 °C for 1 hour of time, to evaluate the wear property of the developed hy-

brid composite. Dipti et al., [15] have done an extensive literature survey and have given seven steps for the process of optimal progress of mechanical-tribological properties. The involvement of these properties depends on the following steps. (i) Choice of the matrix material and suitable reinforcing agent, in consideration to their binding properties has to be chosen. (ii) The volume or weight % addition of the reinforcing agent shows an imperative part in improving the possessions of the composite. Certain value of calculated reinforcement addition above the threshold value will deteriorate the overall properties of the composite. (iii) Pre heat treatment for metal alloy for proper property enhancement of the composite. (iv) Adding of all cover flux throughout melting and degasifying (v) pre heat treatment for reinforcement (vi) Manual-motorized stirring, adding of pre-heated reinforcing agent and wetting agent and temperature control of the abrasive slurry. (vii) Pouring the abrasive slurry to pre-heated mould. Andreatta et al., [16] experimented the corrosion behaviour of the AA7075 alloy, which was taken in the cold rolled manner. T6 temperature method was followed for the process of heat treatment. Solution treatment in salt bath was done at $470^{O}C$ for time interval of 1 hour. Quenching was followed by the process of solutionizing which was done in water bath. Artificial treatment for ageing process was done by keeping it in nitrogen environment. The exposition of the developed specimen was not exposed to water to avoid the precipitation of Mg in Mg_2Si. A S B et al., [17] have made a review on aluminum matrix with alumina, Boron carbide and Titanium carbide which are manufactured with the following process respectively; stir-casting, centrifugal-casting and powder-metallurgy. The usage of aluminum and its composites have found a large application in automotive and aerospace sector. Mechanical and microstructure analysis of the developed composites were carried out with and without heat treatment. The microstructure studies of the heat treatment composites reveal that there is a significant change in microstructure of the specimen and the stress are relieved. On the similar lines with previous author C Velmurugan et al., [18], made an experimental and comparative study on Al6061 reinforced with 10 wt % of SiC and varied wt % of 2 and 4 of graphite developed by stir casting method. The comparative study was done with heat treatment and without treatment. The developed specimens were exposed to the temperature of 530 °C for 1 hour followed by water quenching and artificial ageing. Harness and microstructure were carried out and it was found that heat treatment has significant impact on alloy undergone heat treatment. J W Pinto et al., [19] using the method of stir casting has developed hybrid aluminum composite by reinforcing coconut-shell ash particles and E-glass. The study was conducted to analyze the hardness, wear and tensile results for the specimens with and without heat treatment. T.S. Kiran et al., [20] deliberated the wear characters of cast and heat-treated Zinc and aluminum alloy reinforced with graphite and silicon carbide by stir-casting. Heat treatment was done at 370 °C and then quenching in water at room temperature. Artificial ageing was done at 180 °C. It was noted that the wear behavior was optimal for heat treated specimens.

2. Experimental Details

2.1 Matrix material: Al7075 alloy & Reinforcements

Aluminum alloy 7075 was used as matrix-material & Graphite, E-Glass fiber and Mica were utilized as reinforcing materials. Table1 establishes chemical composition of Al7075 alloy. Table 2 shows the various combination of reinforcement used in the present investigation.

Table 1. Composition of Aluminum 7075 alloys

Element	Cu	Cr	Mn	Mg	Si	Ti	Zn	Fe	Al
Wt %	1.8	0.2	0.4	1.9	0.5	0.15	3.25	0.5	Balance

2.2 Synthesis of Hybrid composites

The hybrid composite was manufactured by casting process by melting Aluminum 7075 alloy at 800°C. Entrapped gases were removed from liquid aluminum alloy utilizing hexa-chloro-ethane tablets (C_2C_{16}). Degassed and preheated graphite, E-Glass fiber and Mica were transferred to liquid metal which is agitated at 400 rpm. The reinforcement was added to the molten metal while the stirring is continued so that they get dispersed evenly in the melt. Varied percentage of the particles was added to melt. The liquefied Al7075 melt with graphite, E-Glass fiber and Mica elements are agitated for 10 minutes thus to ensure that the scattering is even. The cast-iron die used for casting, Solidified alloy and composites are then machined to obtain the test samples for various tests.

Table 2. Hybrid Reinforcement Combinations

Sl. No.	Mica (wt %)	Graphite (wt %)	E-Glass fiber (wt %)	Sl. No.	Mica (wt %)	Graphite (wt %)	E-Glass fiber (wt %)
1	0	0	0	**25**	2	0	2
2	0	1	0	**26**	2	1	2
3	0	3	0	**27**	2	3	2
4	0	5	0	**28**	2	5	2
5	1	0	0	**29**	3	0	2
6	1	1	0	**30**	3	1	2
7	1	3	0	**31**	3	3	2
8	1	5	0	**32**	3	5	2
9	2	0	0	**33**	0	0	4
10	2	1	0	**34**	0	1	4
11	2	3	0	**35**	0	3	4
12	2	5	0	**36**	0	5	4
13	3	0	0	**37**	1	0	4
14	3	1	0	**38**	1	1	4
15	3	3	0	**39**	1	3	4
16	3	5	0	**40**	1	5	4
17	0	0	2	**41**	2	0	4
18	0	1	2	**42**	2	1	4
19	0	3	2	**43**	2	3	4
20	0	5	2	**44**	2	5	4
21	1	0	2	**45**	3	0	4
22	1	1	2	**46**	3	1	4
23	1	3	2	**47**	3	3	4
24	1	5	2	**48**	3	5	4

2.3 Heat Treatment

Aluminum 7075 alloy and its composites samples were machined to the required size and subjected to heat treatment process (i.e. T6 condition) in a heat treatment furnace. The examples were solutionised at 500 °C for 2 hours and quenched in room temperature water. Ageing was carried out both naturally and artificially at 190 °C from 0 Hours to 9 Hours for all the test samples.

2.4 Grain size analysis

Grain size and Image examination was completed according to ASTM 112-96 standard test procedure on polished tests of Al7075 alloy and its hybrid composites utilizing Clemex Image-Analyzer software.

2.5 X-ray diffraction studies (XRD)

Philips X'Pert Pro X-ray diffractometer was used for taking X-ray diffraction patterns on developed hybrid composites using Cu-Kαradiation at BMS college of Engineering, Bangalore.

2.6 Hardness

Brinell hardness equipment was utilized to evaluate the brinel hardness value of the alloy and composite. Evaluation was performed on the surface of the polished alloy and composite. Five indentations were made on each composition to circumvallate effect of hard secondary particles at a constant load of ten kilo grams. Different regions and areas were covered during the evaluation. All five values were reflected to obtain the final value of the hardness. The Brinel Hardness number is premeditated conferring to the succeeding formulation.

2.7 Tensile test

Tensile properties of the alloy and hybrid composites were determined suing a universal testing machine of capacity 10 ton driven with servo driven hydraulic based system. Specimens were loaded parallel to the direction of loading. The proportionality of the stress and strain is represented as hooks law which is a primary section of the stress and strain curve. Gradual increase in the load was applied and equivalent strain was recorded. When load is detached, without generating the long-lasting plastic deformation elastic limit was the value where higher stress was observed in the material. After this there was rapid expansion of the stress value without any appreciable increase in strain value. Without any recognizable increase in the load the samples was deformed and extreme stress was recorded at yield point.

3. Results and Discussions

3.1 Microstructure

In the present work, Mechanical properties like, Brinell hardness, tensile strength and ductility were studied. In addition to this, Al7075 hybrid composites were also subjected to artificial ageing to check its effect on aforementioned properties. The microstructure and surface analysis in cast, artificial aged, after tensile tested condition was conducted using optical and scanning electron microscopes. The fracture surface was studied to have an idea of mechanisms responsible for fracture of composites. It should be noted that the all the properties obtained Al7075 hybrid composites were compared with Al7075 alloy prepared under same processing and

heat treatment conditions. Optical microscope was used to study the dispersion of reinforcements in the Al7075 matrix and is presented in Fig. 3.1. Here different combinations of three reinforcements namely mica, graphite and E-glass fiber were used to develop Al7075 hybrid composites. Take for instance Figs. 3.1 (a), (d) and (g) shows the microstructure of hybrid composites in which mica content was varied from 1 to 3 % in steps of 1 %, graphite content was fixed to 1 % and E-glass content was 0 %. In these cases the mica and graphite particles were hardly visible in optical microstructure. This is due to the fact that the mica and graphite particle content is quite small enough to capture in optical microscope. Few particles belonging of these two reinforcements are seem to be located at the grain boundaries of α-Al and few are located in between the grain boundaries. Figs. 3.1 (b), (e) and (h) shows the microstructure of hybrid composites in which the mica content is varied from 1 to 3 % in the steps of 1 %, graphite content is fixed to 3 % and E-glass fiber content is fixed to 2 %. The microstructure showed large clusters of these reinforcements located at the grain boundaries of α-Al. The clustering was quite predominant in the hybrid composite with 3 % mica, 3 % graphite and 2 % E-glass fiber which is shown in Fig.3.1 (h). Finally the Figs. 3.1 (c), (f) and (i) shows the microstructure of hybrid composites in which the mica content is varied from 1 to 3 % in the steps of 1 %, graphite content is fixed to 5 % and E-glass fiber content is fixed to 4 %. Unlike in the optical images shown in Figs. 3.1 (b), (e) and (h), here the clustering was not observed indicating good dispersion of reinforcements.

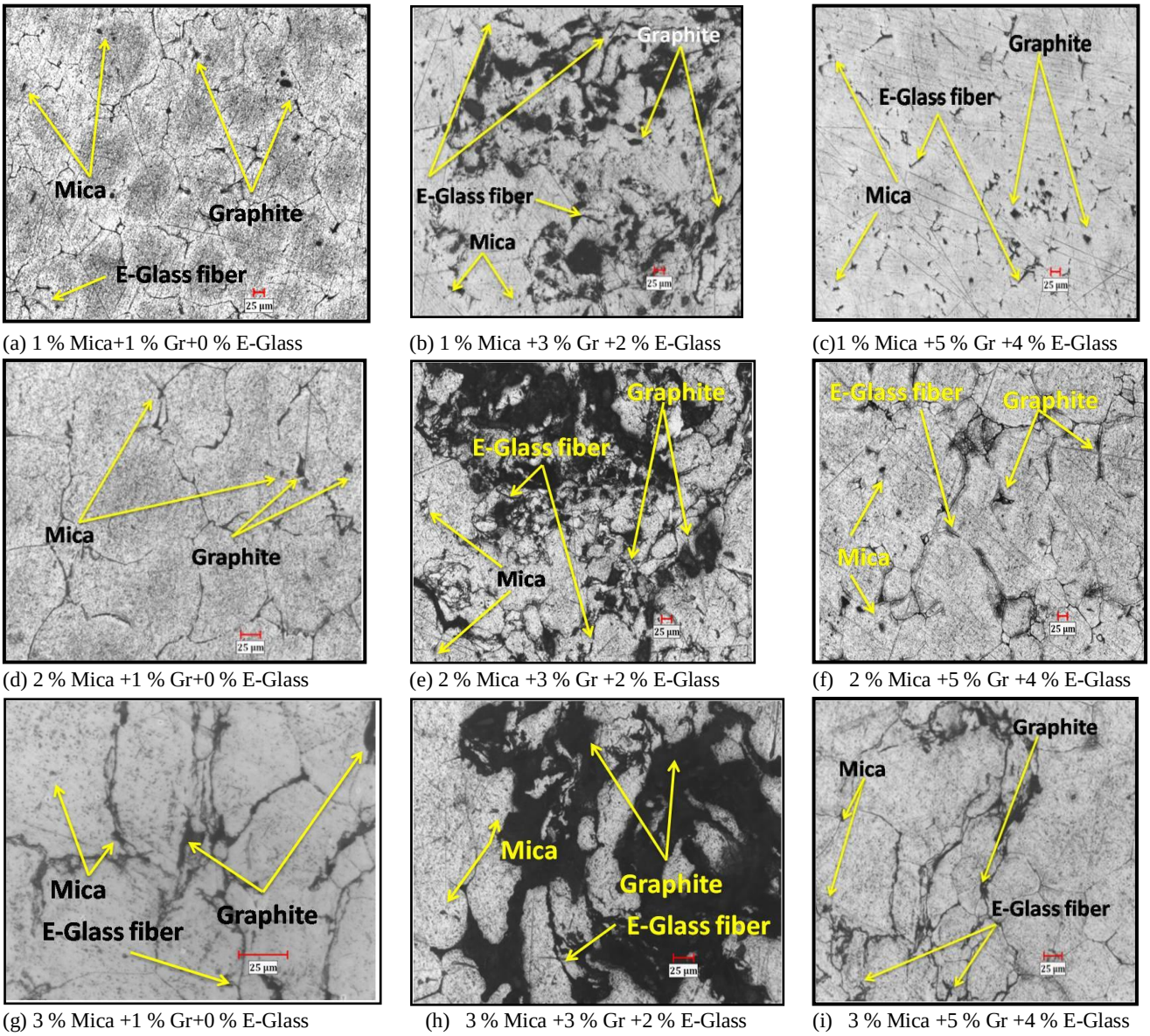

(a) 1 % Mica+1 % Gr+0 % E-Glass (b) 1 % Mica +3 % Gr +2 % E-Glass (c)1 % Mica +5 % Gr +4 % E-Glass

(d) 2 % Mica +1 % Gr+0 % E-Glass (e) 2 % Mica +3 % Gr +2 % E-Glass (f) 2 % Mica +5 % Gr +4 % E-Glass

(g) 3 % Mica +1 % Gr+0 % E-Glass (h) 3 % Mica +3 % Gr +2 % E-Glass (i) 3 % Mica +5 % Gr +4 % E-Glass

Fig. 3.1. Optical micrographs of Al7075 hybrid composites with varying weight percentage of reinforcements

Most of reinforcement particles are found to be located at the grain boundaries and some of them pinned in between the grain boundaries. The dispersion of reinforcements is very important from performance point of view because this factor influence the mechanical as well other properties. For good properties and performance of composites the reinforcement should be uniformly dispersed in the matrix. There are number of possibilities in which the reinforcements can alter the microstructure of Al7075 matrix. Some of them are, the reinforcements can trigger the heterogeneous nucleation of new grains in the melt, influence the fluidity of the melt, influence the grain size and influence the coarsening of dendrite arm. One can observe that in all cases with the increase in reinforcement content the grain size is found to decrease considerably. Take for example, the microstructure of hybrid composites shown in Figs. 3.1 (c), (f) and (i) depicts that the grain size was quite bigger in case of Fig. 3.1 (c) which has mica content of 1 % while when it is increased to 3 % the grain size tends to decrease considerably. However one need to quantify the grain size to know how much decrement can be obtained by increasing the mica content. This is done by obtaining the average grain size and analyzing them, which is presented in detail in upcoming section. At present the surface analysis is presented here which tells that the grain size of hybrid composites is lesser when the reinforcement content is increased. The possibility of decrease in grain size is attributed to the presence of reinforcements which acts as heterogeneous nucleation sites is well supported by the research findings reported by Sujith et al. [21]. The authors reported the development of TiC reinforced Al7079 composites developed by stir casting process. Here the reinforcing phase TiC particles acted as nucleating sites for solidification of α-Al in the melt during solidification. The solidifying α-Al will have fine size when compared to the Al7075 alloy in unreinforced condition.

The presence of reinforcements at the grain boundaries or inside the grains is depends on their density and the viscosity of moving solidification interface. The particles tend to float or settle done in the melt or there is high possibility of pushed by moving solid-liquid interface. By observing the optical micrographs it is presumed that the final factor is quite predominant. The moving solidification interface tend to push the low density reinforcements like graphite and E-glass fibers in last freezing interdendritic melt or entrapped between the solidifying interface which forms the grain boundaries. This is why most of the reinforcements are found at the grain boundaries rather inside grains. Optical images of solutionized and aged Al7075 hybrid composites are presented in the Fig. 3.2. The ageing duration of hybrid composites is varied from 1 to 9 hours in the step of 2 hours and resulting microstructure is shown in Figs. 3.2 (a), (d) and (g) shows the microstructure of heat treated hybrid composites in which mica content was varied from 1 to 3 % in steps of 1 %, graphite content was fixed to 1 % and E-glass content was 0 %. From Fig 3.2 it can be observed that the $MgZn_2$ and Al_2CuMg phases are segregated into the interdendritic spaces. In several cases the $MgZn_2$ phase is found at the interface between the reinforcements and Al7075 matrix. But in present case no such observations were made and the zones with less distribution of $MgZn_2$ and Al_2CuMg phases are known to be precipitate free zone. Figs. 3.2 (b), (e) and (h) shows the microstructure of heat treated hybrid composites in which the mica content is varied from 1 to 3 % in the steps of 1 %, graphite content is fixed to 3 % and E-glass fiber content is fixed to 2 %. Similar to previous case the $MgZn_2$ and Al_2CuMg phases formed after heat treatment were found to be in the interior of dendrite arms. One can see the distribution of both the intermetallic compounds was random in the microstructure. Figs. 3.2 (c), (f) and (i) shows the microstructure of hybrid composites in which the mica content is varied from 1 to 3 % in the steps of 1 %, graphite content is fixed to 5 % and E-glass fiber content is fixed to 4 %. Similar to previous reinforcement combinations here also the $MgZn_2$ and Al_2CuMg phases were seen in the microstructure. The two intermetallic compounds were found to be randomly dispersed and mostly located in the interdendritic spaces. Although one should be able to observe that the number density of these two phases is quite higher than that of previous two cases. It is well known that when the Al7075 alloy or its composites is subjected to the solution treatment which is followed by rapid cooling which otherwise is known as quenching. During this the precipitation takes place however it is not instantaneous and for that ageing is carried out. With ageing time the precipitation keeps on increasing until the solution approaches to equilibrium composition thereafter the precipitation stops. During ageing time following precipitation sequence takes place, supersaturated solid-solution followed by Guinier-Preston zones followed by semi-coherent $MgZn_2$ and finally equilibrium precipitate, η-$MgZn_2$.

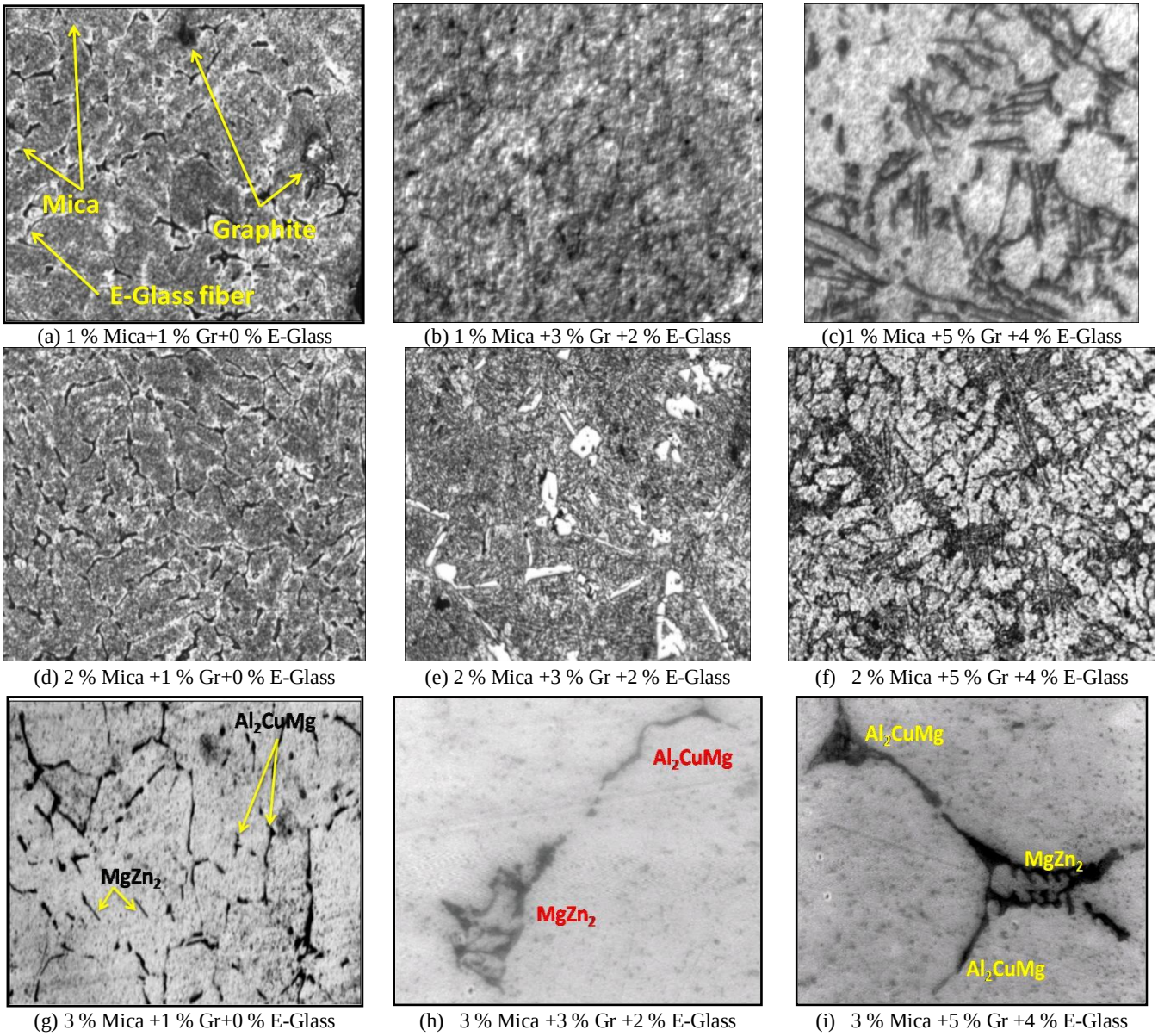

(a) 1 % Mica+1 % Gr+0 % E-Glass (b) 1 % Mica +3 % Gr +2 % E-Glass (c)1 % Mica +5 % Gr +4 % E-Glass

(d) 2 % Mica +1 % Gr+0 % E-Glass (e) 2 % Mica +3 % Gr +2 % E-Glass (f) 2 % Mica +5 % Gr +4 % E-Glass

(g) 3 % Mica +1 % Gr+0 % E-Glass (h) 3 % Mica +3 % Gr +2 % E-Glass (i) 3 % Mica +5 % Gr +4 % E-Glass

Fig. 3.2. Optical micrographs of Al7075 hybrid composites age hardened at (a, b, c) 5 hours, (d, e, f) 7 hours and (g, h, i) 9 hours

However, nucleation of these precipitates largely depends upon the Zn/Mg ratio which should not exceed 2.2 to form $MgZn_2$ precipitates. Nucleation of these precipitates can be random or homogeneous in specific regions like grain boundaries and vacancies. Although by observing interdendritic spaces the formation of $MgZn_2$ and Al_2CuMg phases have been confirmed up to certain extent but in order to have complete clarification the use of XRD would be quite helpful. The XRD studies on before and after heat treatment of Al7075 hybrid composites is conducted to know the possible composition of precipitates. But the most important thing to be considered here is morphology, dispersion and size of the precipitates which influence the mechanical and thermal considerably. However, in general η'-$MgZn_2$ is responsible for strengthening of Al7075 alloy and its hybrid composites. This metastable semicoherent phase η'-$MgZn_2$ is formed by replacing metastable GP zones because of low interfacial energy of the latter [22, 23]. Compared to the optical images of Al7075 hybrid composites in Figs. 3.1 & 3.2, the overall grain structure after heat treatment didn't experience any significant changes. In their work, Leacock et al [24, 25] studied the mechanical properties of naturally aged Al7075 alloy. They found out that the grain structure of the alloy didn't change after solution heat treatment. The observations made from Figs.3.1 and 3.2 in the present work is well supported by this research findings were no significant changes were observed in the optical images of Al7075 hybrid composites before and after heat treatment.

3.2 Grain Size Analysis

When the matrix phase transformation is considered it is well known that the grain size is much smaller in composites compared to that of their monolithic counterparts. Presence of reinforcement particles enhances the nucleation of recrystallized grains and help in pinning the grain boundaries during grain growth. So it becomes very much necessary to understand the effect of three different reinforcements on the Al7075 grain size. Effect of varying reinforcement content on grain size of Al7075 matrix is shown in Fig. 3.3 and 3.4. Here two different cases are presented, first case is related to effect of reinforcement content and second case is related to effect of heat treatment on average grain size of the Al7075 hybrid composites.

3.2.1 Effect of reinforcements

In this section effect of varying reinforcements on average grain size of Al7075 hybrid composites is presented in Fig. 3.3. Here three graphical representations are made in which the content of E-glass fiber is fixed to 0, 2 and 4 % in each graph while the mica (1–3 %) and graphite content (1–5 %) is varied in Al7075 hybrid composites. In first graphical representation shown in Fig. 3.3 (a), the content of E-glass fiber content is fixed 0 % while that of mica (1–3 %) and graphite content (1–5 %) is varied. Take the case of Al7075 alloy without reinforcements, the average grain size is found to be ~64 μm, however with the addition of 1 , 2 and 3 % mica, the average grain sizes are ~58 μm, ~53 μm and ~44 μm respectively for Al7075/mica composites. With the addition of 3 % mica, the decrease in grain size is about 31.25 % when compared to that of unreinforced Al7075 alloy. In another case the composite with 5 % graphite showed average grain size of ~60 μm, further with the addition of 1, 2 and 3 % mica, the average grain sizes are ~53 μm, ~40 μm and ~35 μm respectively for Al7075/mica/graphite hybrid composites. With the addition of 3 % mica and 5 % graphite, the decrease in grain size is about 45.31 % when compared to that of unreinforced Al7075 alloy. It should be noted that this is the case were E-glass fiber content is 0 % and the composite contains only mica and graphite particles. Overall one can observe that increase in reinforcement content the average grain size of Al7075 matrix tends to decrease considerably. In second graphical representation shown in Fig. 3.3 (b), the content of E-glass fiber content is fixed 2 % while that of mica (1–3 %) and graphite content (1–5 %) is varied. As mentioned previously the average grain size of Al7075 alloy without reinforcements was found to be ~64 μm, however with the addition of 2 % E-glass fiber, the average grain size was ~66 μm. In case of hybrid composite where the E-glass fiber content was fixed to 2 % and when the mica content is increased from 1, 2 and 3 % mica the grain sizes were ~56, ~46 and ~43 μm respectively. With the addition of 3 % mica and 2 % E-glass fiber, the decrease in grain size is about 32.81 % when compared to that of unreinforced Al7075 alloy. In another case, the composite with 5 % graphite and 2 % E-glass fiber showed average grain size of ~56 μm, further with the addition of 1, 2 and 3 % mica, the average grain sizes are ~51, ~38 and ~35 μm respectively for Al7075/mica/graphite/E-glass fiber hybrid composites. With the addition of 3 % mica, 5 % graphite and 2 % E-glass fiber, the decrease in grain size is about 45.31 % when compared to that of unreinforced Al7075 alloy. It should be noted that this is the case where E-glass fiber content is 2 % and the composite contains varying mica (1–3 %) and graphite particles (1–5 %). Overall, one can observe that increase in reinforcement content the average grain size of Al7075 matrix tends to decrease significantly. In third graphical representation shown in Fig. 3.3 (c), the content of E-glass fiber content is fixed 4 % while that of mica (1–3 %) and graphite content (1–5 %) is varied. As mentioned previously the average grain size of Al7075 alloy without reinforcements was found to be ~64 μm, however with the addition of 4 % E-glass fiber, the average grain size was ~64 μm. In first hybrid composite where the E-glass fiber content was fixed to 4 % and when the mica content is increased from 1, 2 and 3 % mica the grain sizes were ~55, ~44 and ~42 μm respectively. With the addition of 3 % mica and 4 % E-glass fiber, the decrease in grain size is about 34.37 % when compared to that of unreinforced Al7075 alloy. In another case, the composite with 5 % graphite and 4 % E-glass fiber showed average grain size of ~56 μm, further with the addition of 1, 2 and 3 % mica, the average grain sizes are ~46, ~36 and ~34 μm respectively for Al7075/mica/ graphite/E-glass fiber hybrid composites. With the addition of 3 % mica, 5 % graphite and 4 % E-glass fiber, the decrease in grain size is about 46.87 % when compared to that of unreinforced Al7075 alloy. It should be noted that this is the case were E-glass fiber content is 4 % and the composite contains varying mica (1–3 %) and graphite particles (1–5 %).

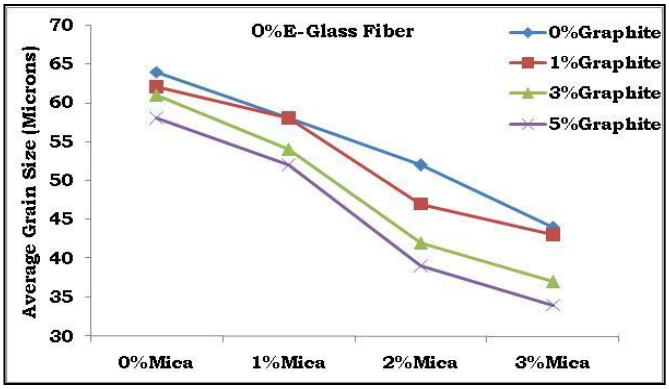

Fig. 3.3a. Variation of grain size with Graphite for 0 % E-Glass fiber

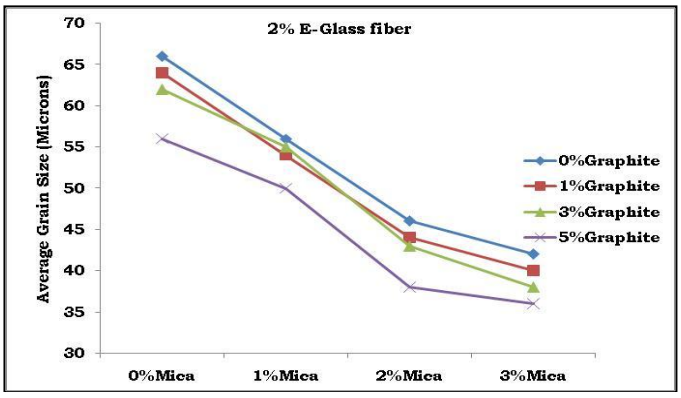

Fig. 3.3b. Variation of grain size with Mica for 2 % E-glass fiber

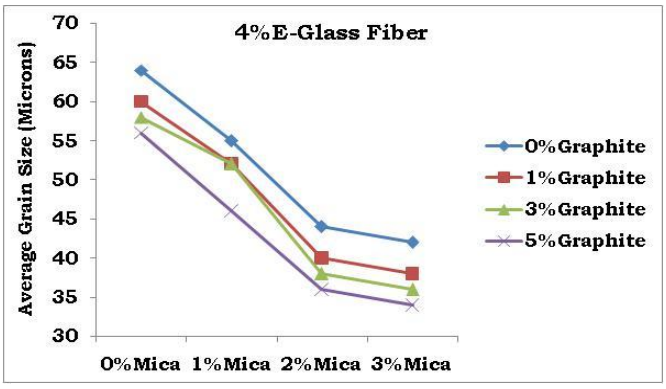

Fig. 3.3c. Variation of grain size with graphite for 4 % E-glass fiber

Overall, one can observe that increase in all the three reinforcement content the average grain size of Al7075 matrix tends to decrease considerably. The main reason for decrease in grain size of Al7075 matrix is attributed to addition of reinforcements which not only retard the α-Al grain growth but also help in nucleating new grains. Rate of α-Al grain growth tends to decrease with the increase in percentage of reinforcements. The obtained results are well in line with those reported by Ramkumar et al [26] on AA7075/TiC composites. The AA7075 matrix was refined due to the addition of TiC particles and pinned the α-Al matrix grains. With the increase in TiC particle content the authors observed decrease in grain size which was supported the crystallographic characteristics in which composites showed high percentage of high angle grain boundaries than AA7075 alloy.

3.2.2 Effect of heat treatment

In this section effect of heat treatment on average grain size of Al7075 hybrid composites is presented in Fig.3.4. Here three graphical representations are made in which the content of E-glass fiber is fixed to 0, 2 and 4 % in each graph while the mica (1–3 %) and graphite content (1–5 %) is varied in Al7075 hybrid composites. In first graphical representation shown in Fig. 3.4(a), the content of E-glass fiber content is fixed 0 % while that of mica (1–3 %) and graphite content (1–5 %) is varied. Take the case of Al7075 alloy without reinforcements, the average grain size is found to be ~61.5 µm, however with the addition of 1, 2 and 3 % mica, the average grain sizes are ~56, 45 and 44 µm respectively for Al7075/mica composites. With the addition of 3 % mica, the decrease in grain size is about 28.45 % when compared to that of unreinforced Al7075 alloy. In another case the composite with 5 % graphite showed average grain size of ~57 µm, further with the addition of 1, 2 and 3 % mica, the average grain sizes are ~49.5, ~37 and ~33 µm respectively for Al7075/mica/graphite hybrid composites. With the addition of 3 % mica and 5 % graphite, the decrease in grain size is about 46.34 % when compared to that of unreinforced Al7075 alloy. It should be noted that this is the case were E-glass fiber content is 0 % and the composite contains only mica and graphite particles. Overall one can observe that increase in reinforcement content the average grain size of Al7075 matrix tends to decrease considerably. In second graphical representation shown in Fig. 3.4(b), the content of E-glass fiber content is fixed 2 % while that of mica (1–3 %) and graphite content (1–5 %) is varied. As mentioned previously the average grain size of Al7075 alloy without reinforcements was found to be ~61.5 µm, however with the addition of 2 % E-glass fiber, the average grain size was 64.5 µm. In first hybrid composite where the E-glass fiber content was fixed to 2 % and when the mica content is increased from 1, 2 and 3 % mica the grain sizes were ~52, ~45 and ~44 µm respectively. With the addition of 3 % mica and 2 % E-glass fiber, the decrease in grain size is about 28.45 % when

compared to that of unreinforced Al7075 alloy. In another case, the composite with 5 % graphite and 2 % E-glass fiber showed average grain size of ~57.5 μm, further with the addition of 1, 2 and 3 % mica, the average grain sizes are ~47.5, ~36.5 and ~31.5 μm respectively for Al7075/mica/graphite/E-glass fiber hybrid composites. With the addition of 3 % mica, 5 % graphite and 2 % E-glass fiber, the decrease in grain size is about 48.78 % when compared to that of unreinforced Al7075 alloy. It should be noted that this is the case were E-glass fiber content is 2 % and the composite contains varying mica (1–3 %) and graphite particles (1–5 %). Overall one can observe that increase in reinforcement content the average grain size of Al7075 matrix tends to decrease considerably. In third graphical representation shown in Fig. 3.4(c), the content of E-glass fiber content is fixed 4 % while that of mica (1–3 %) and graphite content (1–5 %) is varied. As mentioned previously the average grain size of Al7075 alloy without reinforcements was found to be ~61.5 μm, however with the addition of 4 % E-glass fiber, the average grain size was ~63 μm. It should be noted that this is the case were E-glass fiber content is 4 % and the composite contains varying mica (1–3 %) and graphite particles (1–5 %). When compared to the grain sizes prior to heat treatment, the values were as high as several hundred microns. For instance unreinforced Al7075 had grain sizes of ~240 μm and ~61.5 μm for before and after heat treatment conditions respectively. One can see that the grain refinement is quite significant which is attributed to grain boundary pinning by the presence of $MgZn_2$ and Al_2CuMg precipitates. After heat treatment the precipitates formed in matrix which is either present at the grain boundaries or at the triple junctions tends to pin the grains from growing. In addition to this, the precipitates tend to interact more with dislocations by reducing their mobility in terms of driving force [27–28]. The reduced dislocation mobility due to presence of precipitates is one of the fundamental reasons for significant grain refinement in case of heat treated Al7075 alloy and its hybrid composites.

3.3 X-ray Diffraction Analysis (XRD)

It is necessary to understand the phases formed in the unreinforced Al7075 alloy and its hybrid composites before and after heat treatment. In this regard, X-ray diffraction patterns of aforementioned materials were taken and each peak was identified to check which element or compounds were formed. Fig. 3.5 (a), (b) and (c) shows the XRD patterns for Al7075 alloy, Al7075/3 %mica/5 %graphite/4 %E-glass hybrid composite before and after heat treatment. In case of unreinforced Al7075 alloy, the XRD pattern as shown in Fig.3.5 (a) shows the face centered cubic phase Al as major element. Since Al is the parent element in Al7075 alloy all the three peaks observed in XRD pattern were of Al. Absence of other alloying elements like Mg, Si or Cu can be attributed to their low weight percentage in the complete alloy which is also the limitation of X-ray to detect phases which are well below 2 % volume fraction. The XRD pattern of Al7075/3 %mica/5 %graphite/4 %E-glass hybrid composite shown in Fig. 3.5 (b) corresponds to prior heat treatment. It can be seen that the three peaks corresponding to Al were seen at 38º, 46º and 65º 2θ angles. Small peaks related to all the three reinforcement mica, graphite and E-glass fiber were also observed in the XRD pattern. It is confirm that all the main constituents of hybrid composites were present and by observing peaks it seems that they are in crystalline condition. Finally, Fig. 3.5 (c) shows the XRD pattern of heat treated Al7075/3 %mica/5 %graphite/4 %E-glass hybrid composite. Large peaks corresponding to Al were seen at 38º, 46º and 65º 2θ angles while various small peaks of all the three reinforcements were also seen. In addition to these, two more intermetallic compounds were seen the XRD pattern. These intermetallic compounds were related to $MgZn_2$ and Al_2CuMg phases which are generally formed after heat treatment. As mentioned in previous section, these phases are generally found in the interdendritic spaces and are formed during solution treatment. Appropriate low ageing temperature results in nucleation of these two phases while in medium ageing temperature the coarsening and at very high temperature the dissolution of these phases occurs. Fig. 3.5 (c) supports the claim made in microstructure analysis towards the formation of $MgZn_2$ and Al_2CuMg phases. Previous investigations have shown that the $MgZn_2$ phase is formed when the Zn/Mg ratio in the Al7075 alloy exceeds 2.2.

On the other hand, the Al_2CuMg phase is nucleated during non-equilibrium solidification process. In some cases this phase tend to disappear when the solution treatment of Al7075 exceeds more than 10 hours. Similarly the Mg $(Cu, Al, Zn)_2$ content tends to decrease with the increase in solution temperature and time [25]. The distribution and size of these two phases dictate the mechanical properties of heat treated Al7075 and its hybrid composites.

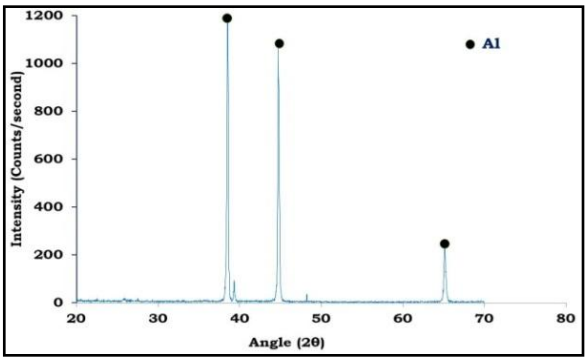

Fig. 3.5a. X-ray diffraction pattern of cast Al7075

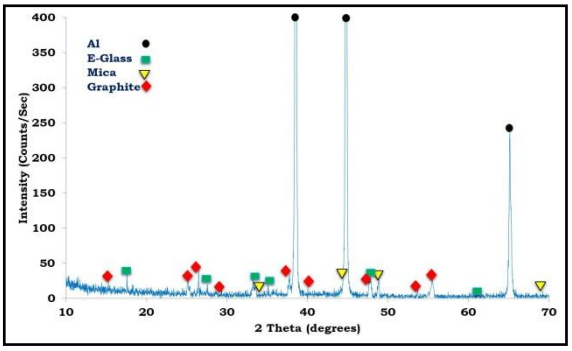

Fig. 3.5b. X-ray diffraction pattern of cast Al7075 based hybrid composite prior to heat treatment

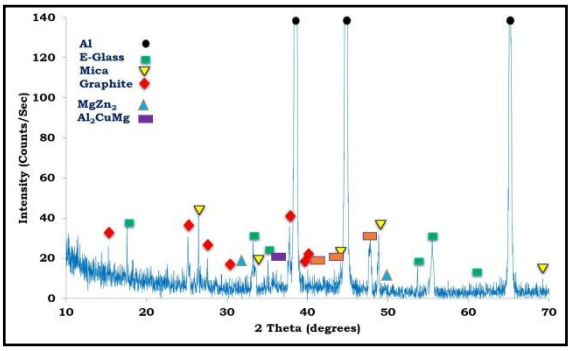

Fig. 3.5c. X-ray diffraction pattern of cast Al7075 based hybrid composite after heat treatment

3.4 Ultimate Tensile strength

In this section effect of varying reinforcements and heat treatment on ultimate tensile strength of Al7075 alloy and its hybrid composites is presented in Fig. 3.6 (a)–(d).

3.4.1 Effect of reinforcements

Effect of varying reinforcements on ultimate tensile strength of Al7075 alloy and its hybrid composites is presented in Fig.3.6 Here, three graphical representations are made in which the content of E-glass fiber is fixed to 0 %, 2 % and 4 % in each graph while the mica (1–3 %) and graphite content (1–5 %) is varied in Al7075 hybrid composites. In first graphical representation shown in Fig. 3.6(a), the content of E-glass fiber content is fixed 0 % while that of mica (1–3 %) and graphite content (1–5 %) is varied. Take the case of Al7075 alloy without reinforcements, the ultimate tensile strength is found to be 143 MPa, however with the addition of 1, 2 and 3 % mica, the ultimate tensile strength is increased to 152, 182 and 230 MPa respectively for Al7075/mica composites. With the addition of 3 % mica, the increase in ultimate tensile strength is about 60.83 % when compared to that of unreinforced Al7075 alloy. In another case the composite with 5 % graphite showed ultimate tensile strength of 248 MPa, further with the addition of 1, 2 and 3 % mica, the ultimate tensile strength values are increased to 255, 263 and 322 MPa respectively for Al7075/mica/graphite hybrid composites. With the addition of 3 % mica and 5 % graphite, the increase in yield strength is about 225.17 % when compared to that of unreinforced Al7075 alloy. In this case the E-glass fiber content is 0 % and the composite contains only mica and graphite particles. Overall, one can observe that increase in reinforcement content the ultimate tensile strength of Al7075 matrix tends to increase significantly. In second graphical representation shown in Fig. 3.6(b), the content of E-glass fiber content is fixed 2 % while that of mica (1–3 %) and graphite content (1–5 %) is varied. As mentioned previously the ultimate tensile strength of Al7075 alloy without reinforcements was found to be 143 MPa, however with the addition of 2 % E-glass fiber, the ultimate tensile strength was increased to 152 MPa. In case of hybrid composite where the E-glass fiber content was fixed to 2 % and when the mica content is increased from 1, 2 and 3 % mica the ultimate tensile strength values were increased to 159, 191 and 225 MPa respectively. With the addition of 3 % mica and 2 % E-glass fiber, the increase in ultimate tensile strength value is about 57.34 % when compared to that of unreinforced Al7075 alloy. In another case, the composite with 5 % graphite and 2 % E-glass fiber showed ultimate tensile strength of 265 MPa, further with the addition of 1, 2 and 3 % mica, the ultimate tensile strength values were to 265, 276 and 333 MPa respectively for Al7075/mica/graphite/E-glass fiber hybrid composites. With the addition of 3 % mica, 5 % graphite and 2 % E-glass fiber, the increase in ultimate tensile strength is about 232.86 % when compared to that of unreinforced Al7075 alloy. It should be noted that this is the case were E-glass fiber content is 2 % and the composite contains varying mica (1–3 %) and graphite particles (1–5 %).

Overall, one can observe that increase in reinforcement content the ultimate tensile strength of Al7075 matrix tends to increase significantly when compared with that of unreinforced Al7075 alloy. In third graphical representation shown in Fig. 3.6 (c), the content of E-glass fiber content is fixed 4 % while that of mica (1–3 %) and graphite content (1–5 %) is varied. As mentioned previously the ultimate tensile strength of Al7075 alloy without reinforcements was found to be 143 MPa, however with the addition of 4 % E-glass fiber, the ultimate tensile strength increased to 158 MPa. In first case the hybrid composite where the E-glass fiber content was fixed to 4 % and when the mica content is increased from 1, 2 and 3 % mica the ultimate tensile strength increased to 165, 200 and 230 MPa respectively. With the addition of 3 % mica and 4 % E-glass fiber, the increase in ultimate tensile strength value is about 60.83 % when compared to that of unreinforced Al7075 alloy. In another case, the composite with 5 % graphite and 4 % E-glass fiber showed ultimate tensile strength of 271 MPa, further with the addition of 1, 2 and 3 % mica, the ultimate tensile strength values were 280, 291 and 335 MPa respectively for Al7075/mica/graphite/E-glass fiber hybrid composites. With the addition of 3 % mica, 5 % graphite and 4 % E-glass fiber, the increase in ultimate tensile strength is about 234.26 % when compared to that of unreinforced Al7075 alloy. It should be noted that this is the case were E-glass fiber content is 4 % and the composite contains varying mica (1–3 %) and graphite particles (1–5 %). Overall one can observe that increase in all the three reinforcement content the ultimate tensile strength of Al7075 matrix tends to increase significantly.

3.4.2 Effect of heat treatment

In this section the effect of heat treatment on tensile strength of Al7075 alloy and its composites is presented in Fig. 3.6 (d). In the case of unreinforced Al7075 alloy, the tensile strength before and after heat treatment was 143 and 156 MPa respectively. For Al7075/3 %mica composite, the tensile strength before and after heat treatment was 230 and 267 MPa respectively. For Al7075/5 %graphite composite, the tensile strength before and after heat treatment was 274 and 275 MPa respectively. Finally, for Al7075/3 %mica/5 %graphite/4 %E-glass fiber hybrid composite, the tensile strength before and after heat treatment was 335 and 341 MPa respectively. One can see that after heat treatment the tensile strength of all materials were found to increase substantially. The increase in tensile strength values is mainly due to the formation of $MgZn_2$ and Al_2CuMg precipitates. As mentioned in the yield strength section, the tensile strength increases due to the fact that the precipitates formed in the Al7075 matrix tend to interact more with dislocations and reduce their mobility in terms of driving force. The dislocations are bowed around $MgZn_2$ and Al_2CuMg precipitate and then reconnect forming a loop around the precipitates. The stress required will be higher in heat treated materials because of dislocation movement hindering by precipitates than that of materials which aren't heat treated [29]. Due to this the tensile strength of both Al7075 alloy and its hybrid composites is increased significantly. Increase in reinforcement content the number of heterogeneous nucleation sites in the composites will be higher which helps in formation of more number of $MgZn_2$ and Al_2CuMg precipitates. This is one reason that the composites with higher reinforcement content had higher tensile strength than that of composites with lower reinforcement content. Overall, the precipitation strengthening is main reason for increment in strength in case of heat treated materials when compared to that of untreated materials.

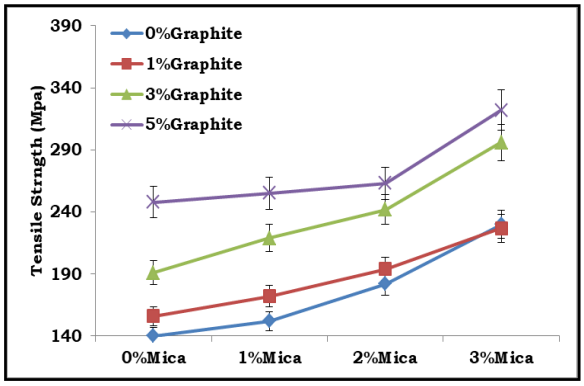

Fig. 3.6a. Variation of UTS w.r.t. weight % of mica at 0 %E-Glass fiber

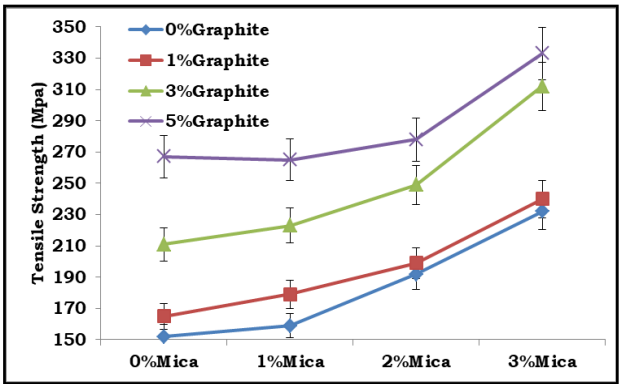

Fig. 3.6b. Variation of UTS w.r.t. weight % of mica at 2 %E-Glass fiber

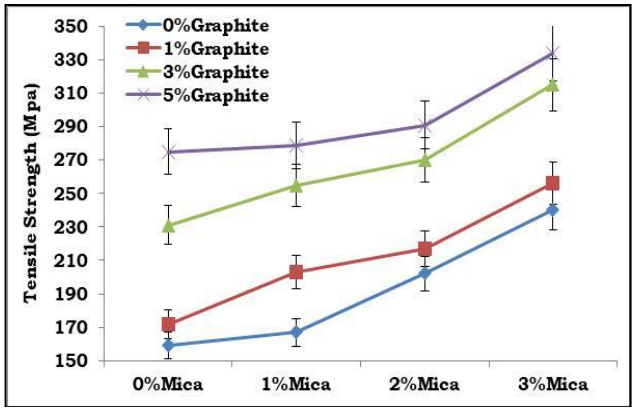

Fig. 3.6c. Variation of UTS w.r.t. weight % of mica at 4 %E-Glass fiber

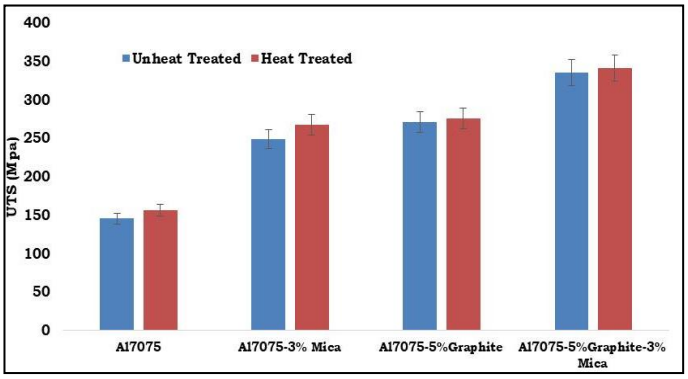

Fig. 3.6d. Effect of heat treatment on Ultimate Tensile Strength for 4 %E-Glass fiber

3.4.3 Strengthening Mechanisms

The increment in ultimate tensile strength of Al7075 alloy and its hybrid composites before and after heat treatment is due to Hall-Petch strengthening, load transfer strength, thermal mismatch strengthening and precipitation strengthening [30-32]. Here each strengthening is discussed one by one to understand how they influence the strength of Al7075 alloy and its hybrid composites. It is well known that all the composites showed substantial decrement in grain size when compared to that of unreinforced Al7075 alloy. It is shown that, the grain size of Al7075 matrix tends to decrease with the increase in reinforcement content. Due to increase in grain boundary density the composites especially the one with higher mica, graphite and E-glass fiber content showed higher strength values. This is mainly because the grain boundaries provide utmost resistance to the dislocation motion because the lattice disorder is very high at the grain boundary region. Further according to Hall-Petch equation where it describes that grain size is inversely proportional to strength of materials. One can see that with the grain refinement and decrease in grain size the composites shows improvement in strength values. Second strengthening mechanism is load transfer which largely depends on the interface between reinforcements and Al7075 matrix. As shown in Fig. 3.1, the reinforcements were found to be dispersed uniformly in the Al7075 matrix with good interfacial bonding. The interface between the reinforcements and the matrix was found to clean and unwanted reaction was not seen which is confirmed by the XRD patterns taken on the composites. Due to this the load transfer from Al7075 matrix to hard reinforcements is quite efficient and effective which contributes to increment in strength of composites. Higher the reinforcement content, higher is the load borne by the reinforcements which is why the composites with higher reinforcement content showed higher strength values. It is well known that the coefficient of thermal expansion is different for different materials. In present case mismatch in coefficient of thermal expansion between matrix ($25.2 \times 10^{-6}\ K^{-1}$) and reinforcements is very high. Due to this the dislocation density is higher in composites when compared to that of unreinforced Al7075 alloy. Because of this high compressive stress is generated and dislocation tangles are formed which create large stress contrast. Such phenomena taking place at the matrix/reinforcement interface benefits the strength values of Al7075 composites. With the increase in reinforcement content the density of dislocations tends to increase several folds due to which the strength values are increased significantly. Finally the precipitation hardening is quite elaborately mentioned in individual yield and ultimate tensile strength sections. After heat treatment, $MgZn_2$ and Al_2CuMg precipitates are formed in the both Al7075 alloy and its composites. The formation of precipitates is confirmed in both microstructures and in XRD patterns. The formation of precipitates contributes via hindering the dislocation motion as well as slowing them down. With the increase in number of reinforcements and their content the number density of precipitates tend to increase significantly. Due to this the strength of Al7075 alloy and its composites tends to increase substantially. Overall the increment in strength of composites is due to combined effect of all strengthening mechanisms.

3.4.5 Tensile Fracture Surface Analysis (Before heat treatment)

After tensile test, the fractured specimen of both untreated and heat treated Al7075 composites where

subjected to SEM analysis to evaluate the fracture mechanisms operating. The SEM micrographs showing the fractured surface are shown in Figs. 3.7 and 3.8 for untreated and heat treated samples. The fracture of the samples is highly influenced by the shape, size and dispersion of the reinforcements, in this case mica, graphite and E-glass fiber. The examination is done to understand whether the fracture is brittle or ductile and to see the fracture initiation site.

0 %E-Glass fiber

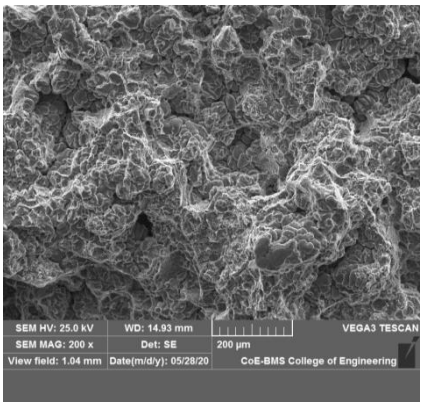

(a)Al7075-5 % Graphite

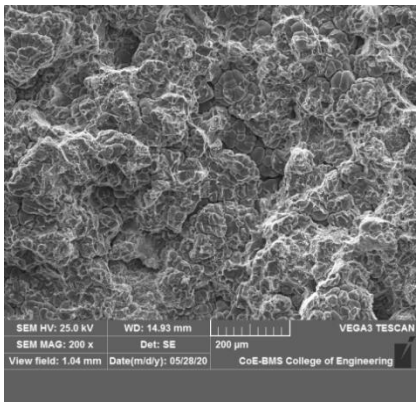

(b)Al7075-3 %Mica

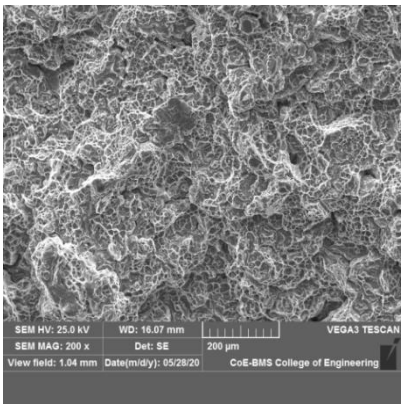

(c)Al7075-5 % Graphite -3 %Mica

2 %E-Glass fiber

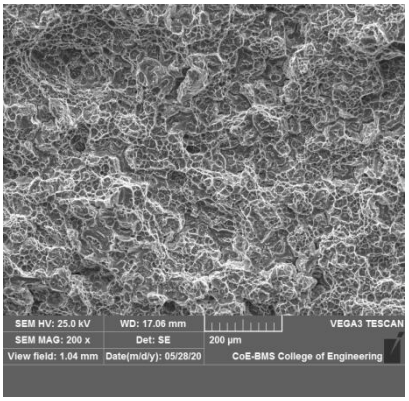

(d)Al7075-5 % Graphite

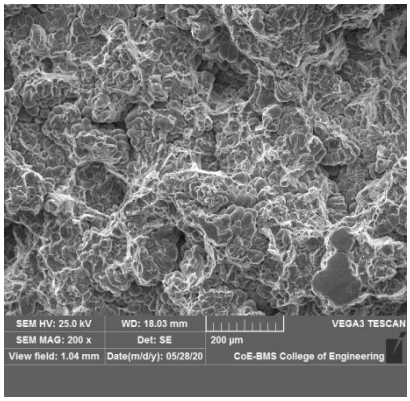

(e)Al7075-3 %Mica

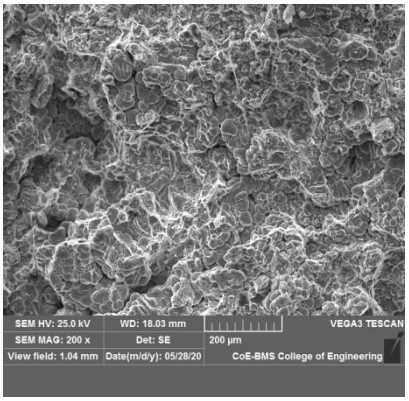

(f)Al7075-5 % Graphite -3 %Mica

4 %E-Glass fiber

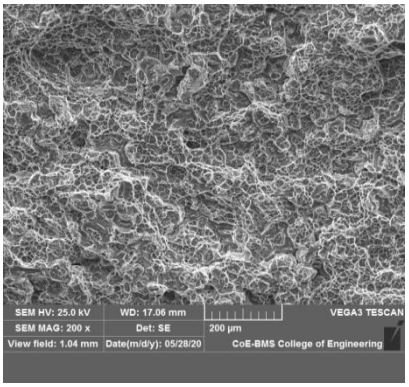

(g)Al7075-5 %Graphite

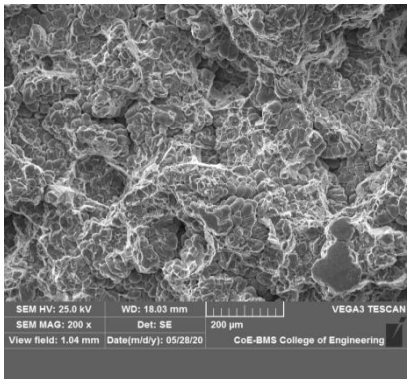

(h)Al7075-3 %Mica

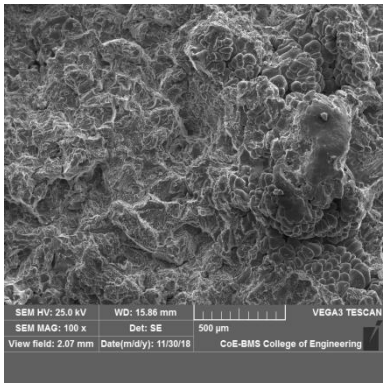

(i)Al7075-5 % Graphite-3 %Mica

Fig. 3.7(a-i) Tensile Fracture Surface Analysis (Before heat treatment)

The SEM micrographs of Al7075 composites with varying E-glass fiber content prior to heat treatment are shown in Fig. 3.7 (a)–(i). In the first case E-glass fiber content is 0 % while the composites contain 5 %graphite, 3 %mica and 5 %graphite/3 %mica (see Fig. 3.7 (a)–(c)). The fracture surface of composites showed typical shrinkage porosity formed during stir casting process. The cracks are seen originating from the shrinkage porosity and extending to dimples. The porosity typically acts as nucleating sites for the cracks during tensile loading and keeps extending to Al7075matrix. Here, the extension of crack and its

propagation through the entire matrix largely depends upon the pores present in other parts. Percentage of shrinkage porosity is higher in case of 5 %graphite and 5 %graphite/3 %mica reinforced Al7075 composites as shown in Fig. 3.7 (a) and (c). The number and size of the dimples formed on the fracture surface dictates the ductility of the unreinforced alloy or composites [35]. However, it is seen from see Fig. 3.7 (a)–(c) that the composites consisted of coarse size lesser number of dimples. This implies that all the composites have reasonable ductility and in case of hybrid composites poor ductility as seen in Fig. 5.12 (a) and (c). In the second case the E-glass fiber content is 2 % while the composites contain 5 %graphite, 3 %mica and 5 %graphite/3 %mica (see Fig. 3.7 (d)–(f)). Here in this case of composites, the shrinkage porosities are seen in the fracture surfaces. The number of dimples is very less as compared to previous case of composites where the E-glass fiber content was 0 %. With the addition of E-glass fiber the number of dimples was reduced and there was no protrusion of dimples. This observation directly provides evidence that the composites have lower elastic deformation and poor ductility. Finally, when the E-glass fiber content is increased to 4 % while the composites containing 5 %graphite, 3 %mica and 5 %graphite/3 %mica showed large number of shrinkage porosity (see Fig. 3.7 (g)–(i)). The depth of the shrinkage porosity observed in the fracture surface ran into several hundred microns. See the SEM image Fig. 3.7 (i) of Al7075/3 %mica/5 %graphite/4 %E-glass fiber whose fracture surface showed very large shrinkage porosity whose depth was several hundred microns. Most of the shrinkage porosity is formed during solidification of composites where sufficient molten metal was not available to compensate for the shortage. These shrinkage porosities encourage initiation of cracks and propagate them through the other defects present in the Al7075 matrix. Further similar cracks are initiated at the large number of interfaces due to presence of higher content of E-glass fiber. The cracks initiated at the porosities and interfaces tend to enhance the crack propagation rate and cause the failure of composites. The presence of few and coarse size dimples explains that increase in E-glass fiber content the ductility of composites is compromised. Although the matrix is ductile but presence of large number of interfaces do facilitate the crack propagation and plays no role in arresting the cracks. The presence of large number of interfaces changes the mode of fracture from ductile mode for Al7075 alloy to brittle mode for Al7075 composites [33].

3.4.6 Tensile Fracture Surface Analysis (After heat treatment)

The SEM micrographs of Al7075 composites before and after heat treatment are shown in Fig. 3.8 (a)–(f). First let take the case of Al7075/5 %graphite composite before and after heat treatment whose fracture surface is shown in the Fig. 3.8 (a) and (b). It can be seen that the both the fracture surfaces showed similar cause of failure that is shrinkage porosity. During casting lack of molten metal flow to the last freezing area can lead to the formation of shrinkage porosity. The formation of cracks in the porosity region especially near the dendrites can be clearly seen in the Fig. 3.7 (b). Large amount of porosity is seen in fractured surface which is one of the main causes for initiation of cracks. The cracks formed then tends to propagate such similar regions and finally leading to a stage where the applied stress becomes unbearable for the materials which leads to failure. At few places in the fracture surface debonding of graphite particles from the Al7075 matrix is also seen. It is well known that the graphite particles are generally has poor wettability with the molten metals. Due to its poor wettability there is gap the interface. Such weak interfaces also facilitate the crack nucleation and contribute to the crack propagation. Overall, for Al7075/5 %mica composite before and after heat treatment the main reason for fracture is shrinkage porosity. Considering the case of Al7075/3 %mica composite before and after heat treatment the fracture surface as presented in the Fig. 3.8 (c) and (d) showed the main reason for failure as shrinkage porosity. Similar to previous composite case, here in case of mica reinforced composites the shrinkage porosity is found to be the major reason for the failure as the features consisted of large pores. The cracks formed at the dendritic region where porosity is predominant propagates through the adjacent such weak regions and cause failure. One can see that both the fracture surface hardly showed formation any kind of dimples which is main characteristic of brittle failure. One can presume that the failure is mainly brittle in nature since the interfaces formed between matrix/reinforcement encourages crack propagation due to which the ductile matrix is unable to arrest the crack. Finally the SEM micrograph showing the fracture surface of Al7075/3 %mica/5 %graphite composites before and after heat treatment is shown in Fig. 3.8 (e) and (f). The fracture surface showed absence of dimples which is characteristic of unreinforced Al7075 alloy. From this it

can be considered that with the addition of multiple reinforcements the ductile nature of Al7075 matrix tends to transform to brittle nature. This is mainly due to work hardening of matrix by the addition of reinforcements. Due to this the plastic strain is generated surrounding the reinforcements as well as around the precipitates. This is the reason because of which composites display plastic deformation rather than elastic deformation which otherwise seen in unreinforced Al7075 alloy. So one can see that in case of composites before and after heat treatment, the presence of multiple reinforcements present in soft ductile matrix tend to pose constraint in the deformation and limits the elastic deformation due to which they tends to fail in brittle mode with major contribution from shrinkage porosity [34, 35].

Unheat Treated

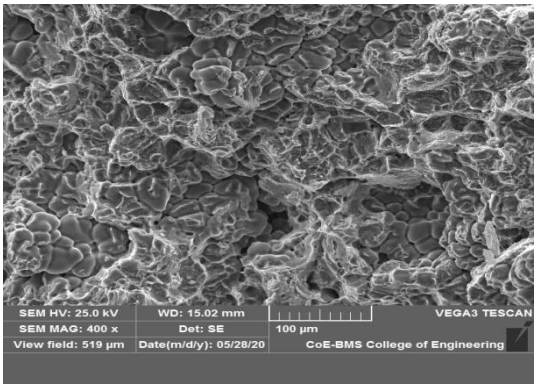

(a)Al7075-5 %Graphite

Heat Treated

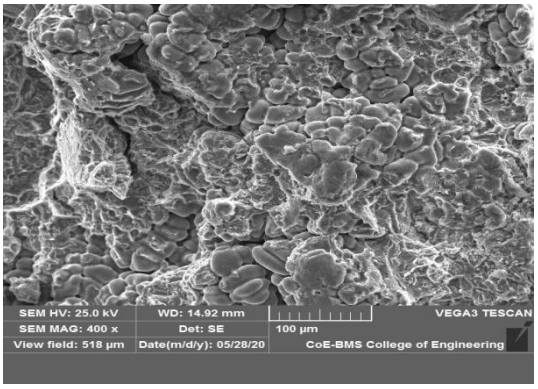

(b)Al7075-5 %Graphite

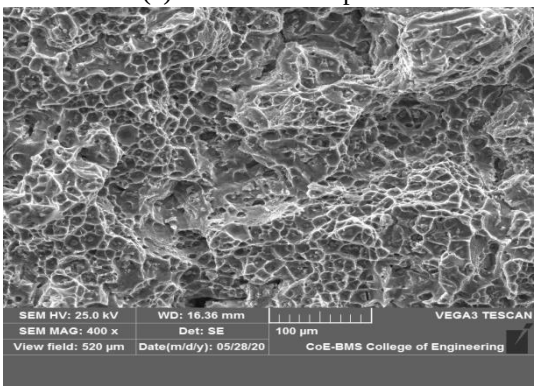

(c)Al7075-3 %Mica

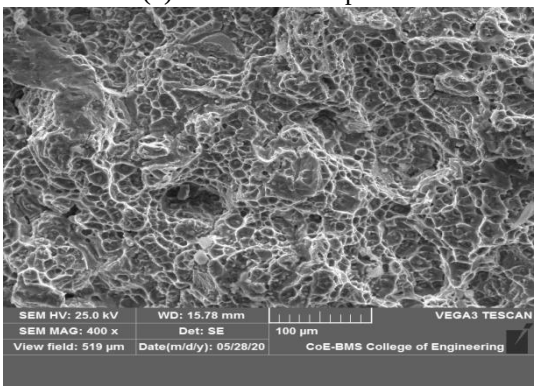

(d)Al7075-3 %Mica

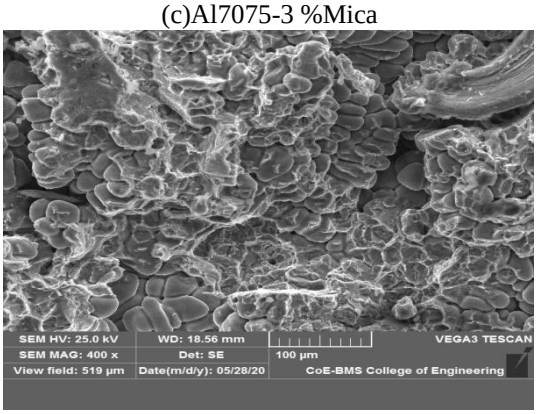

(e)Al7075-5 % Graphite -3 %Mica

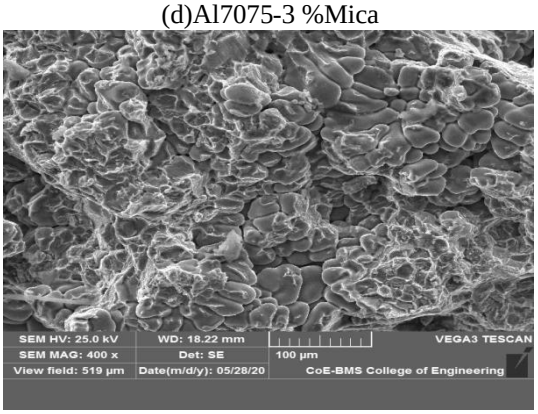

(f)Al7075-5 % Graphite -3 %Mica

Fig. 3.8(a–f) Tensile Fracture Surface Analysis (After heat treatment)

3.5 Hardness

Here, two different cases are presented, first case is related to effect of reinforcement content and second case is related to effect of heat treatment on Brinell hardness of the Al7075 hybrid composites.

3.5.1 Effect of reinforcements

In this section effect of varying reinforcements on average hardness value of Al7075 hybrid composites is presented in Fig. 3.9. Here, three graphical representations are made in which the content of E-glass

fiber is fixed to 0, 2 and 4 % in each graph while the mica (1–3 %) and graphite content (1–5 %) is varied in Al7075 hybrid composites. In first graphical representation shown in Fig. 5.6 (a), the content of E-glass fiber content is fixed 0 % while that of mica (1–3 %) and graphite content (1–5 %) is varied. Take the case of Al7075 alloy without reinforcements, the average hardness value is found to be 68 BHN, however with the addition of 1, 2 and 3 % mica, the average hardness values are 69, 81 and 87 BHN respectively for Al7075/mica composites. With the addition of 3 % mica, the increase in hardness is about 27.94 % when compared to that of unreinforced Al7075 alloy. In another case the composite with 5 % graphite showed hardness value of 71 BHN, further with the addition of 1, 2 and 3 % mica, the hardness values are 79, 97 and 103 BHN respectively for Al7075/mica/graphite hybrid composites. With the addition of 3 % mica and 5 % graphite, the increase in hardness is about 51.47 % when compared to that of unreinforced Al7075 alloy. In this case the E-glass fiber content is 0 % and the composite contains only mica and graphite particles. Overall, one can observe that increase in reinforcement content the average hardness values of Al7075 matrix tends to increase significantly. In second graphical representation shown in Fig. 3.9 (b), the content of E-glass fiber content is fixed 2 % while that of mica (1–3 %) and graphite content (1–5 %) is varied. As mentioned previously the average hardness value of Al7075 alloy without reinforcements was found to be 68 BHN, however with the addition of 2 % E-glass fiber, the average hardness value was increased to 71 BHN. In case of hybrid composite where the E-glass fiber content was fixed to 2 % and when the mica content is increased from 1, 2 and 3 % mica the hardness values were 72, 85 and 91 BHN respectively. With the addition of 3 % mica and 2 % E-glass fiber, the increase in hardness value is about 33.82 % when compared to that of unreinforced Al7075 alloy. In another case, the composite with 5 % graphite and 2 % E-glass fiber showed average hardness value of 79 BHN, further with the addition of 1, 2 and 3 % mica, the average hardness values were increased to 81, 95 and 108 BHN respectively for Al7075/mica/graphite/E-glass fiber hybrid composites. With the addition of 3 % mica, 5 % graphite and 2 % E-glass fiber, the increase in hardness value is about 58.82 % when compared to that of unreinforced Al7075 alloy. It should be noted that this is the case were E-glass fiber content is 2 % and the composite contains varying mica (1–3 %) and graphite particles (1–5 %). Overall one can observe that increase in reinforcement content the average hardness value of Al7075 matrix tends to increase significantly when compared with that of unreinforced Al7075 alloy.

In third graphical representation shown in Fig. 3.9 (c), the content of E-glass fiber content is fixed 4 % while that of mica (1–3 %) and graphite content (1–5 %) is varied. As mentioned previously the average hardness value of Al7075 alloy without reinforcements was found to be 68 BHN, however with the addition of 4 % E-glass fiber, the average hardness value was 72 BHN. In first hybrid composite where the E-glass fiber content was fixed to 4 % and when the mica content is increased from 1, 2 and 3 % mica the hardness value were increased to 74, 87 and 92 BHN respectively. With the addition of 3 % mica and 4 % E-glass fiber, the increase in hardness value is about 35.28 % when compared to that of unreinforced Al7075 alloy. In another case, the composite with 5 % graphite and 4 % E-glass fiber showed average hardness value of 79 BHN, further with the addition of 1, 2 and 3 % mica, the average hardness values were increased to 83, 99 and 111 BHN respectively for Al7075/mica/ graphite/E-glass fiber hybrid composites. With the addition of 3 % mica, 5 % graphite and 4 % E-glass fiber, the increase in hardness value is about 63.23 % when compared to that of unreinforced Al7075 alloy. It should be noted that this is the case were E-glass fiber content is 4 % and the composite contains varying mica (1–3 %) and graphite particles (1–5 %). Overall one can observe that increase in all the three reinforcement content the average hardness value of Al7075 matrix tends to increase significantly. The increase in hardness depends mainly on dispersion of reinforcements in the matrix and their strengthening ability. For good mechanical performance the dispersion of reinforcements is very important aspect in the hybrid composites. When the reinforcements are uniformly dispersed in the matrix material than the possibility of resistance to plastic deformation against indentation is very high. In present case there are three different reinforcements which are found to be uniformly dispersed in the Al7075 matrix. So when the indentation is made, than the plastic deformation experiences resistance due to presence of these reinforcements. This is the reason why hybrid composites have higher Brinell hardness than that of Al7075 alloy. In addition to this the increase in reinforcement content whether it could E-glass fiber from 0–4 % or mica from 1–3 % or

graphite content from 1–5 % also increased the hardness of resulting hybrid composites. With increase in more number of reinforcements than there is high possibility that these are placed quite closely to each other due to which the indenter finds it difficult to cause large plastic deformation. A closer look on the work reported by Javdani and Daei-sorkhabi [36] explains that the result presented by the current work is well in line with that reported by these authors. In their work the authors claimed that the increase in hardness value of Al7075/B_4C composite was attributed to uniform dispersion of B_4C particles. The uniform dispersion was achieved during processing period and this facilitated in efficient load transfer from Al7075 matrix phase to the B_4C particles.

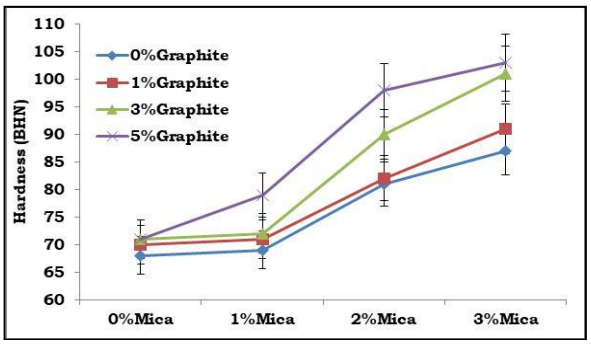

Fig. 3.9a. Variation of hardness with respect to mica at 0 %E-glass fiber

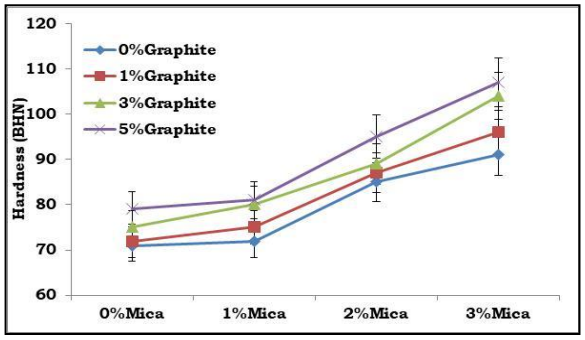

Fig. 3.9b. Variation of hardness with respect to mica at 2 %E-glass fiber

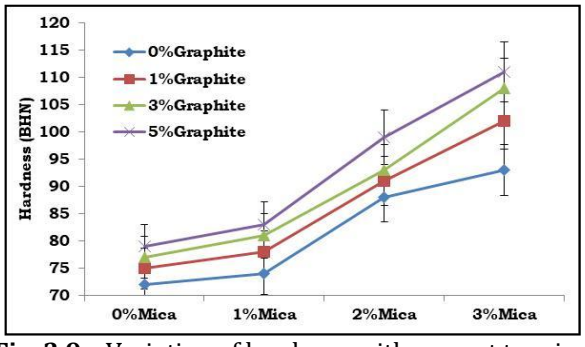

Fig. 3.9c. Variation of hardness with respect to mica at 4 %E-glass fiber

3.5.2 Effect of ageing duration

Ageing duration was varied from 1 to 9 hours in the step of 2 hours to check its effect on hardness of Al7075 alloy, Al7075/3 %Mica,4 %E-glass, Al7075/5 %graphite/4 %E-glass and Al7075/4 %E-glass/3 %Mica/5 %graphite fiber composites and is shown in Fig.3.10. To start with, the hardness of Al7075 alloy tends to increase with the increase in ageing duration but until 7 hours. After ageing duration of 7 hours, the hardness tends to decrease when the duration is extended to 9 hours. The hardness of Al7075 alloy at 1, 7 and 9 hours are 69, 73 and 67 BHN respectively. One can see that peak hardness for Al7075 alloy was achieved when the ageing duration in about 7 hours. Similarly hardness of Al7075/4 %E-glass/3 %Mica/5 %graphite composite tends to increase with the increase in ageing duration but until 7 hours. The hardness of Al7075/4 %E-glass/3 %Mica/5 %graphite composites at 1, 7 and 9 hours are 86, 92 and 90 BHN respectively. The increase in ageing duration from 1 to 7 hours increased the hardness of Al7075/4 %E-glass/3 %Mica/5 %graphite composite however the hardness tends to decrease beyond 7 hours. During ageing time the precipitation sequence will be supersaturated solid-solution followed by Guinier-Preston zones, semi-coherent $MgZn_2$ and finally equilibrium precipitate, η-$MgZn_2$. In present case, the hybrid composites as shown in optical microstructure showed the presence of Al_2CuMg and $MgZn_2$ phases. Although formation of these precipitates help in improving properties via precipitation hardening but the size and distribution of these precipitates plays an important role here. When the Al_2CuMg and $MgZn_2$ phases are finer and smaller in size they help in improving hardness of Al7075 alloy and its hybrid composites. But as soon as thermodynamic equilibrium is reached the relatively larger precipitates tend to grow and smaller one tends to shrink. Growing of precipitates is highly dependent on the temperature and at high temperatures the atoms tends move faster and initiate for coarsening.

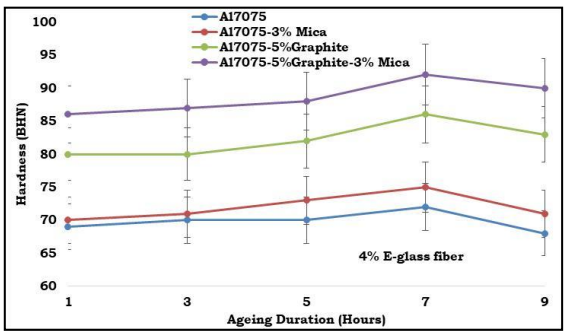

Fig. 3.10. Effect of ageing duration on hardness

Due to this the precipitates begin to coarse and no longer contribute to increment in hardness. This is the reason why the Al7075 alloy or hybrid composites which are aged for longer time durations such as 9 hours tend to suffer from precipitate coarsening and poor hardness values. On the other hand the finer size and uniform dispersion of Al_2CuMg and $MgZn_2$ phases with appropriate spacing between themselves help in achieving peak hardness at 7 hours of ageing.

3.5.3 Effect of heat treatment

In this section effect of heat treatment on average hardness value of Al7075 hybrid composites is presented in Fig. 3.11. The ageing duration was fixed to 7 hours based on the ageing duration test conducted on fewer samples of Al7075 alloy and composites which is shown in Fig. 3.10. Here three graphical representations are made in which the content of E-glass fiber is fixed to 0 %, 2 % and 4 % in each graph while the mica (1–3 %) and graphite content (1–5 %) is varied in Al7075 hybrid composites. In first graphical representation shown in Fig. 3.11 (a), the content of E-glass fiber content is fixed 0 % while that of mica (1–3 %) and graphite content (1–5 %) is varied. In case of Al7075 alloy without reinforcements, the average hardness value is found to be 71 BHN, however with the addition of 1, 2 and 3 % mica, the average hardness values are 73, 88 and 92 BHN respectively for Al7075/mica composites. Here it is observed that after heat treatment the hardness value of Al7075 alloy has increased to 71 BHN compared to untreated stage where it had hardness value of 68 BHN. With the addition of 3 % mica, the increase in hardness value is about 29.57 % when compared to that of unreinforced Al7075 alloy. In another case the composite with 5 % graphite showed average hardness value of 75 BHN, further with the addition of 1, 2 and 3 % mica, the average hardness values are 84, 102 and 109 BHN respectively for Al7075/mica/graphite hybrid composites. With the addition of 3 % mica and 5 % graphite, the increase in hardness value is about 53.52 % when compared to that of unreinforced Al7075 alloy. It should be noted that this is the case were E-glass fiber content is 0 % and the composite contains only mica and graphite particles. Overall one can observe that increase in reinforcement content the average hardness value of Al7075 matrix tends to increase significantly. In second graphical representation shown in Fig. 3.11(b), the content of E-glass fiber content is fixed 2 % while that of mica (1–3 %) and graphite content (1–5 %) is varied. As mentioned previously the average hardness value of Al7075 alloy without reinforcements was found to be 71 BHN, however with the addition of 2 % E-glass fiber, the average hardness value was increased to 74 BHN. In first hybrid composite where the E-glass fiber content was fixed to 2 % and when the mica content is increased from 1, 2 and 3 % mica the hardness values were increased to 78, 90 and 94 BHN respectively. With the addition of 3 % mica and 2 % E-glass fiber, the increase in hardness value is about 32.39 % when compared to that of unreinforced Al7075 alloy in heat treated condition. In another case, the composite with 5 % graphite and 2 % E-glass fiber showed average hardness value of 81 BHN, further with the addition of 1, 2 and 3 % mica, the average hardness values increased to 84, 104 and 112 BHN respectively for Al7075/mica/graphite/E-glass fiber hybrid composites. With the addition of 3 % mica, 5 % graphite and 2 % E-glass fiber, the increase in hardness value is about 57.74 % when compared to that of unreinforced Al7075 alloy. It should be noted that this is the case were E-glass fiber content is 2 % and the composite contains varying mica (1–3 %) and graphite particles (1–5 %). Overall one can observe that increase in reinforcement content the average hardness value of Al7075 matrix tends to increase significantly.

In third graphical representation shown in Fig. 3.11(c), the content of E-glass fiber content is fixed 4 % while that of mica (1–3 %) and graphite content (1–5 %) is varied. As mentioned previously the average hardness value of Al7075 alloy without reinforcements was found to be 71 BHN, however with the addition of 4 % E-glass fiber, the average hardness value increased to 76 BHN. For hybrid composite where the E-glass fiber content was fixed to 4 % and when the mica content is increased from 1, 2 and 3 % mica the hardness value increased to 79, 91 and 94 BHN respectively. With the addition of 3 % mica and 4 % E-glass fiber, the increase in hardness value is about 32.39 % when compared to that of unreinforced Al7075 alloy in heat treated condition. In another case, the composite with 5 % graphite and 4 % E-glass fiber showed average hardness value of 82 BHN, further with the addition of 1, 2 and 3 % mica, the average hardness value were increased to 86, 107 and 115 BHN respectively for Al7075/mica/graphite/E-glass fiber hybrid composites. With the addition of 3 % mica, 5 % graphite

and 4 % E-glass fiber, the increase in hardness value is about 61.97 % when compared to that of unreinforced Al7075 alloy. It should be noted that this is the case were E-glass fiber content is 4 % and the composite contains varying mica (1–3 %) and graphite particles (1–5 %). When compared to the hardness values prior to heat treatment, the hardness values obtained after heat treatment were high. After 7 hours of peak ageing time duration the hardness values of all the materials were significantly improved.

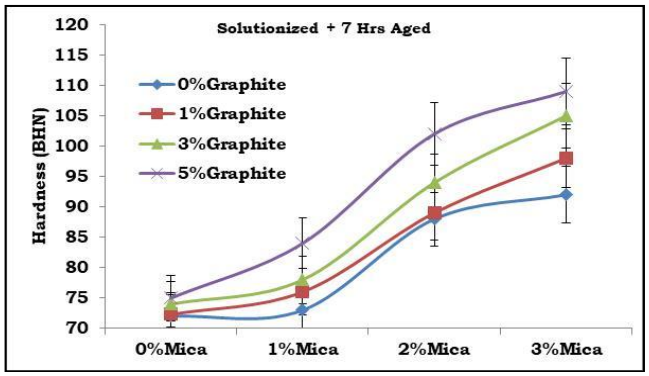

Fig. 3.11a. Variation of hardness with respect to mica at 0 %E-glass fiber

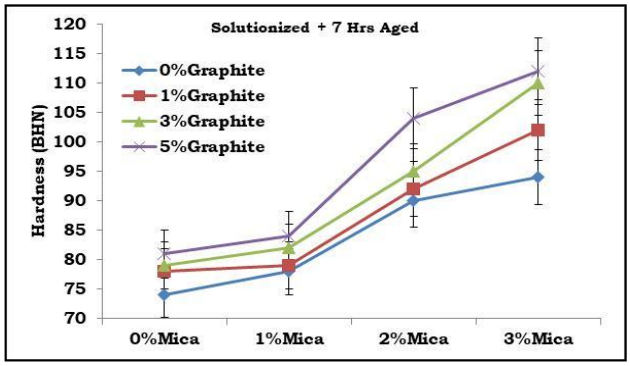

Fig. 3.11b. Variation of hardness with respect to mica at 2 %E-glass fiber

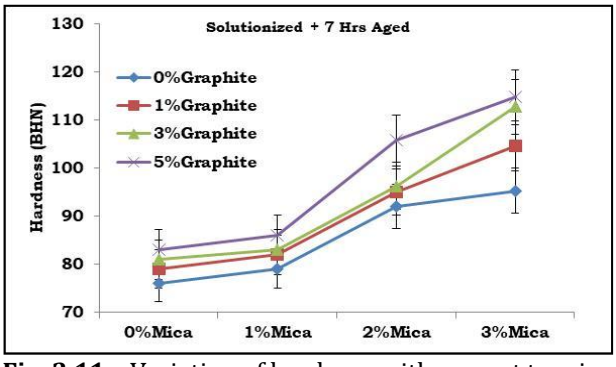

Fig. 3.11c. Variation of hardness with respect to mica at 4 %E-glass fiber

The increase in hardness values is mainly due to the formation of $MgZn_2$ and Al_2CuMg precipitates. These precipitates tend to interact more with dislocations by reducing their mobility in terms of driving force. On the other hand the precipitates which are incoherent with the Al matrix shows Orowan looping mechanism in which dislocations bypass the precipitate by creating a loop around it. If the precipitates are coherent with the Al matrix than the hardness increase results from dislocation shearing of the precipitates [37]. Overall the reduced dislocation mobility due to presence of precipitates is one of the fundamental reasons for significant increase in hardness in case of heat treated Al7075 alloy and its hybrid composites.

Conclusion

The following are the conclusions drawn from the current work,

1. Dispersion of reinforcements (mica, graphite, E-glass fiber) in Al7075 composites was found to be uniform with minimal clustering. Heat treated Al7075 alloy and composites showed formation of $MgZn_2$ and Al_2CuMg phases in the interdendritic regions.
2. X-ray diffraction studies showed no additional peaks apart from Al7075 composite constituents while after XRD patterns after heat treatment confirmed presence of $MgZn_2$ and Al_2CuMg phases.
3. Decrease in grain size of Al7075 matrix was found to decrease with the increase in reinforcements which not only retard the α-Al grain growth but also help in nucleating new grains. After heat treatment grain refinement was attributed to grain boundary pinning by the presence of $MgZn_2$ and Al_2CuMg precipitates.
4. Hardness was found to increase with increase in reinforcement content whether it could E-glass fiber from 0–4 % or mica from 1–3 % or graphite content from 1–5 %. The increase in hardness depends mainly on dispersion of reinforcements in the matrix and their strengthening ability.
5. Post heat treatment the hardness the Al_2CuMg and $MgZn_2$ phases with appropriate spacing between themselves helped in achieving peak hardness at 7 hours of ageing. Reduced dislocation mobility helped in achieving in high hardness.
6. Ultimate tensile strength increased with the increase in reinforcement content both before and after heat treatment. Post heat treatment the increase in yield and ultimate tensile strength was observed which was attributed to the formation of $MgZn_2$ and Al_2CuMg precipitates.

7. The increment in ultimate tensile strength of Al7075 alloy and its composites before and after heat treatment was due to Hall-Petch strengthening, load transfer strength, thermal mismatch strengthening and precipitation strengthening.
8. Change in the mode of fracture from ductile mode for Al7075 alloy to brittle mode for Al7075 composites was observed in tensile fracture analysis conducted using SEM. Post heat treatment studies showed that the presence of multiple reinforcements to pose constraint in the matrix deformation and limits the elastic deformation due to which they tends to fail in brittle mode.

References

[1] Jones D.R.H., Ashby M.F. Engineering Materials-2: An Introduction to Microstructures, Processing and Design. Butterworth-Heinemann, Woburn, UK, 2006, 472 p.

[2] Encyclopedia of composite materials and components. By ed. Martin Gayson. NY, JOHN WILEY & SONS, 1983, 1161 p.

[3] Weeton J.W., Peters D.M., Thomas K.L. Engineers' guide to composite materials. Cleveland, ASM International, 1987, 397 p.

[4] Murthy V.R.S., Jena A.K., Gupta K.P., Murty G.S. Structure and properties of Engineering Materials. New Delhi, Tata McGraw Hill Publishing Company Limited, 2003, 544 p.

[5] Kang C.G., Yoon J.H. The upsetting behavior of semi-solid aluminium material fabricated by a mechanical stirring process. *Journal of Material Production Technology*, 1997, no. 66, pp. 30–38.

[6] Yunsheng Xu, Chung D.D.L. Low-volume-fraction particulate preforms for making metal-matrix composites by liquid metal infiltration. *Journal of Material Science*, 1998, no. 33, pp. 4707–4709.

[7] Chawla N., Chawla K.K. Metal matrix composites. Springer, New York, 2006, 370 p. DOI: https://doi.org/10.1007/978-1-4614-9548-2.

[8] Jamasri, M.W. Wildan, Sulardjaka, Kusnanto. Mechanical Properties of Aluminum Matrix Composite Reinforced by Carbothermally Reduced of Fly Ash. *AIP Conference Proceedings*, 2011, Vol. 1315, no.1, pp. 81–85. DOI: https://doi.org/10.1063/1.3552552.

[9] Jaswinder Singh, Amit Chauhan. Characterization of hybrid aluminum matrix composites for advanced applications – A review. *Journal of Materials Research and Technology*, 2016, Vol. 5, issue 2, pp. 159–169. DOI: https://doi.org/10.1016/j.jmrt.2015.05.004.

[10] Hanumanth G.S., Irons G.A. Particle incorporation by melt stirring for the production of metal-matrix composites. *Journal of Materials Science*, 1993, Vol. 28, issue 9, pp. 2459–2465. DOI: 10.1007/BF01151680.

[11] Siva Prasad D, Shoba C. Hybrid composites – a better choice for high wear resistant materials. *Journal of Materials Research and Technology*, 2014, Vol. 3, no. 2, pp. 172–178. DOI: 10.1016/j.jmrt.2014.03.004.

[12] Kalkanlı A., Durmaz T., Kalemtaş A., Arslan G. Melt Infiltration Casting of Alumina Silicon Carbide and Boron Carbide Reinforced Aluminum Matrix Composites. *Journal of Material Science & Engineering*, 2017, Vol. 6, no. 4. DOI: 10.4172/2169-0022.1000357.

[13] Alaneme K.K., Aluko A. Fracture toughness (K1CK1C) and tensile properties of as-cast and agehardened aluminum (6063)-silicon carbide particulate composites. *Scientia Iranica*, 2012, Vol. 19, no. 4, pp. 992–996.

[14] Song W.Q., Krauklis P, Mouritz A.P., Bandyopadhyay S. The effect of thermal ageing on the abrasive wear behaviour of age-hardening 2014 Al/SiC and 6061 Al/SiC composites. *Wear*, 1995, Vol. 185, Issues 1–2, pp. 125–130. DOI: https://doi.org/10.1016/0043-1648(95)06599-7.

[15] Diptikanta Das, Purna Chandra Mishra, Saranjit Singh, Swati Pattanaik. Fabrication and heat treatment of ceramic-reinforced aluminium matrix composites – a review. *International Journal of Mechanical and Materials Engineering*, 2014, Vol. 9, no. 1. DOI: 10.1186/s40712-014-0006-7.

[16] Andreatta F., Terryn H., Dewit J.H.W. Effect of Solution Heat Treatment on Galvanic Coupling Between Intermetallics and Matrix in AA7075-T6. *Corrosion Science*, 2003, Vol. 45, no. 8, pp. 1733–1746.

[17] Baghel A.S. et al. A Short Review on Effect of Heat Treatment on Microstructure and Mechanical Properties of ADC12/SiC Metal Matrix Composite, *Applied Mechanics and Materials*, 2015, Vol. 813–814, pp. 3–8, DOI: https://doi.org/10.4028/www.scientific.net/AMM.813-814.3.

[18] Velmurugan C. Experimental Study on The Wear Characteristics Of Heat Treated Aluminium Hybrid Composites. *International Journal Of Civil Engineering And Technology*, 2017, Vol., 8, issue 9, pp. 191–200.

[19] Pinto J.W., Sujaykumar G., Sushiledra R.M. Effect of Heat Treatment on Mechanical and Wear Characterization of Coconut Shell Ash and E-glass Fiber Reinforced Aluminum Hybrid Composites. American Journal of Materials Science, 2016, Vol. 6, no. 4A, pp. 15–19. DOI: doi:10.5923/c.materials.201601.03.

[20] Kiran T.S., Prasannakumar M., Basavarajappa S., Viswanatha B.M. Effect of heat treatment on tribological behavior of zinc aluminum alloy reinforced with graphite and SIC particles for journal bearing. *Industrial Lubrication and Tribology*, 2015, Vol. 67, issue 4, pp. 292–300. DOI: https://doi.org/10.1108/ILT-08-2013-0090.

[21] Sujith S.V., Mahapatra M., Mulik R.S. Microstructural characterization and experimental investigations into two body abrasive wear behavior of Al-7079/TiC in-situ metal matrix composites. *Proceedings of the Institution of Mechanical Engineers, Part J: Journal of Engineering Tribology*, 2019, Vol. 234, pp. 588–607. DOI: 10.1177/1350650119883559.

[22] Jacumasso S.C., J.de Paula Martins, A.L.M. de Carvalho. Analysis of precipitate density of an aluminium alloy by TEM and AFM. *REM–International Engineering Journal*, 2016, Vol. 69, no. 4, pp. 451–457. DOI: https://doi.org/10.1590/0370-44672016690019.

[23] Zhang H.B., Wang B., Zhang Y.T., Li Y., He J.L., Zhang Y.F. Influence of aging treatment on the microstructure and mechanical properties of CNTs/7075 Al composites. *Journal of Alloys and Compounds*, 2020, Vol. 814, 152357. DOI: 10.1016/j.jallcom.2019.152357.

[24] Leacock A.G., Howe C., Brown D., Lademo O., Deering A. Evolution of mechanical properties in a 7075 Al-alloy subject to natural ageing. *Materials and Design*, 2013, no. 49, pp. 160–167. DOI: https://doi.org/10.1016/j.matdes.2013.02.023.

[25] Wu H., Wen S., Lu J., Mi Z., Zeng X., Huang H., Nie Z. Microstructural evolution of new type Al−Zn−Mg−Cu alloy with Er and Zr additions during homogenization. *Transactions of Nonferrous Metals Society of China*, 2017, Vol. 27, pp. 1476–1482.

[26] Ramkumar K.R., Sivasankaran S., Al-Mufadi F.A., Siddharth S., Raghu R. Investigations on microstructure, mechanical, and tribological behaviour of AA 7075-x wt. % TiC composites for aerospace applications. *Archives of Civil and Mechanical Engineering*, 2019, no. 19, pp. 428–438.

[27] Nikulin I., Kipelova A., Malopheyev S., Kaibyshev R. Effect of second phase particles on grain refinement during equal-channel angular pressing of an Al–Mg–Mn alloy. *Journal of Materials Science*, 2012, Vol. 60, no. 2, pp. 487–497. DOI: 10.1016/j.actamat.2011.10.023.

[28] Hull D., Bacon D.J. Introduction to Dislocations. Oxford, Butterworth Heinemann, 2011, 272 p.

[29] Gupta R., Chaudhari G.P., Daniel B.S.S. Strengthening mechanisms in ultrasonically processed aluminium matrix composite with in-situ Al_3Ti by salt addition. *Composites Part B: Engineering*, 2018, no. 140, pp. 27–34. DOI: https://doi.org/10.1016/j.compositesb.2017.12.005.

[30] [30] Choi H.J., Shin J.H., Bae D.H. Grain size effect on the strengthening behavior of aluminum-based composites containing multi-walled carbon nanotubes. *Composites Science and Technology*, 2011, no. 71, pp. 1699–1705.

[31] Chen G., Wan J., He N., Zhang H., Han F., Zhang Y. Strengthening mechanisms based on reinforcement distribution uniformity for particle reinforced aluminum matrix composites. *Transactions of Nonferrous Metals Society of China*, 2018, Vol. 28, issue 12, 2395–2400. DOI: https://doi.org/10.1016/S1003-6326(18)64885-X.

[32] Liu X., Liu E., Li J., He C., Zhao N. Investigation of the evolution and strengthening effect of aluminum carbide for in-situ preparation of carbon nanosheets/aluminum composites. *Materials Science & Engineering A*, 2019, Vol. 764, no. 10, pp. 138–139. DOI:10.1016/j.msea.2019.138139.

[33] Pandey V.K., Patel B.P., Guruprasad S. Role of ceramic particulate reinforcements on mechanical properties and fracture behavior of aluminum–based composites. *Materials Science & Engineering A*, 2019, Vol. 745, pp. 252–264. DOI: 10.1016/j.msea.2018.12.030.

[34] McClintock F.A. Ductility, American Society for Metals. *Metals Park*, 1968, pp. 256–261.

[35] Srivatsan T.S., Al-Hajri M., Smith C., Petraroli M. The tensile response and fracture behavior of 2009 aluminum alloy metal matrix composite. *Materials Science and Engineering A*, 2003, Vol. 346, no.1-2, pp. 91–100. DOI:10.1016/S0921-5093(02)00481-1.

[36] Javdani A., Daei-Sorkhabi A.H. Microstructural and mechanical behavior of blended powder semisolid formed Al7075/B_4C composites under different experimental conditions. *Transactions of Nonferrous Metals Society of China*, 2018, Vol. 28, issue 7, pp. 1298–1310. DOI: https://doi.org/10.1016/S1003-6326(18)64767-3.

[37] Ma K., Wen H., Hu T., Topping T.D., Isheim D., Seidman D.N., Lavernia E.J., Schoenung J.M. Mechanical behavior and strengthening mechanisms in ultrafine grain precipitation-strengthened aluminum alloy. Acta Materialia, 2014, Vol. 62, pp. 141–155. DOI: https://doi.org/10.1016/j.actamat.2013.09.042

Received: December 25, 2020